Failure initiation at V-notch tips in quasi-brittle materials

D. Leguillon[1*], Z. Yosibash[2]

[1] Institut Jean le Rond d'Alembert, CNRS UMR 7190, Sorbonne Universités, UPMC Université Paris 06, F-75005 Paris, France.

[2] Computational Mechanics Lab., Dept. of Mechanical Engineering, Ben-Gurion University of the Negev, Beer-Sheva, 84105, Israel.

* corresponding author: dominique.leguillon@upmc.fr

Abstract: At V-notched tips in specimens made of quasi-brittle materials a small damaged or plastic zone is evident that cannot not be neglected in terms of dissipated energy and stress state, although it is small. Herein, to predict the failure initiation at the notch tip, we extend the finite fracture mechanics (FFM) coupled criterion, which requires a simultaneously fulfillment of an energy and a stress criteria.

In the small damaged zone, a damage model is introduced so to decrease the effective Young's modulus in a power law in terms of the distance to the notch tip in such a way that the stress field remains bounded. It seems particularly suited to quasi-brittle materials, since no diffuse damage can occur. This damage zone is coupled to the FFM criterion to provide the necessary condition for failure initiation.

Under the assumption that the damaged zone and the virtual crack extension are small, matched asymptotic expansions are used. It is shown that the damaged zone grows first, proportionally to the square of the applied load and then, above a threshold, a virtual crack of a given length simultaneously satisfies the energy and stress criteria, and failure occurs. The approach allows taking into account varying tensile strength and material toughness in the damaged zone, as may reasonably be expected. Moreover, it is shown that the same coupled stress-energy criterion can directly be applied to quasi-brittle materials by appropriately using the actual material toughness as measured on a cracked specimen.

1. Introduction

The behavior of brittle materials is governed by the elastic Hooke's law until failure. This is obviously an approximation but it has proven to be widely sufficient even if it has something of an anomaly. At some points, called singular, the strain and stress fields tend to infinity. In a 2D homogenous structure this occurs at reentrant corners (Williams, 1959; Leguillon and Sanchez-Palencia, 1987; Yosibash, 2012) (Figure 1).

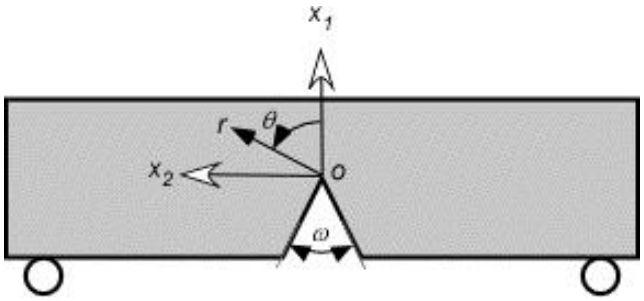

Figure 1. A V-notched specimen made of a homogeneous material - Notations.

In fact, this unbounded growth is the manifestation of an asymptotic solution to the linear equations of elasticity. The displacements, strains and stresses in the vicinity of the notch root take the form

$$\begin{cases} \underline{U}(r,\theta) = \underline{R} + k\ r^{\lambda}\underline{u}(\theta) + \dots \\ \underline{\underline{\varepsilon}}(r,\theta) = k\ r^{\lambda-1}\underline{\underline{e}}(\theta) + \dots \\ \underline{\underline{\sigma}}(r,\theta) = k\ r^{\lambda-1}\underline{\underline{s}}(\theta) + \dots \end{cases} \tag{1}$$

Here, (r,θ) are the polar coordinates with origin at the notch root O. The first term $\underline{R}$ is not of interest and represents a constant vector used for consistency. The strain field $\underline{\underline{\varepsilon}}$ is the symmetric part of the gradient of the displacements $\underline{U}$. The stress tensor $\underline{\underline{\sigma}}$ derives from $\underline{\underline{\varepsilon}}$ according to the Hooke's law. The exponent λ and the associated angular function $\underline{u}(\theta)$ are eigen-pairs to an eigenvalue problem obtained by satisfying the traction free boundary conditions on the V-notch faces (Leguillon and Sanchez-Palencia, 1987) (see Appendix 1). The coefficient k is the generalized stress intensity factor (GSIF) which coincides with the classical mode I stress intensity factor k_I for a crack ($\omega = 0$).

Quasi-brittle materials undergo small (compared to the dimensions of the structure) damage or plastic areas near V-notch tips where the Hooke's law no longer holds true and stresses are not tending to infinity (as in linear elasticity) but are generally bounded. This is also the case

for brittle materials but these areas are so small that in particular the energy dissipation which results from their formation may be neglected. Here, we aim at combining a damage model and a crack initiation criterion to predict failure at V-notches in specimens made of a homogeneous quasi-brittle material. A damage model was proposed in Leguillon (2008) assuming that Young's modulus E evolves following a power law in terms of the distance r to the notch root so that there is no longer a singularity at the corner, i.e. the stress tensor remains bounded. On the other hand, the failure initiation is based on a coupled criterion (Leguillon, 2002) which states that a virtual crack causing failure mutually fulfills two conditions, one is energy driven while the other refers to a stress condition. The drop in potential energy corresponding to the virtual crack formation must exceed the energy that would be consumed to create it, and the tensile stress along the virtual crack must exceed the tensile strength of the material. This coupled criterion has proven effective for predicting failure in many brittle materials and structures such as PMMA and ceramics (Leguillon, 2002; Yosibash et al., 2006), geomaterials (Quesada et al., 2009; Romani et al., 2015), composites (Martin et al., 2010; Martin et al., 2012; Camanho et al., 2012; Garcia et al., 2014; Garcia et al., 2015) and adhesive bonding (Hebel and Becker, 2008; Moradi et al., 2013; Hell et al., 2014).

The outline of this manuscript is as follows. In Section 2, the main ideas of the coupled criterion for brittle materials are summarized. Section 3 is dedicated to the damage model; it describes how the Young modulus changes to accommodate the stress concentration. Asymptotic expansions are used in Section 4 to derive the size of the damage zone as a function of the applied load. The next section is devoted to the identification of a parameter involved in the damage law. Finally, following two different approaches, Sections 6 couples the two models, damage and coupled criterion, to provide a failure criterion for quasi-brittle materials. Numerical results are shown in Section 7 which exhibits comparisons between the different configurations illustrated in Figure 2.

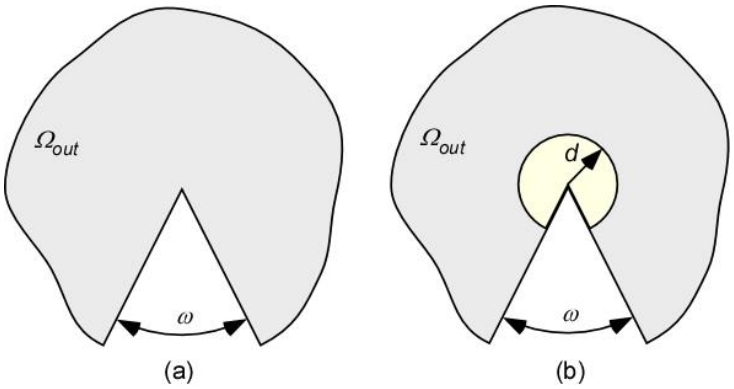

Figure 2. Two different configurations: (a) the sharp V-notch, (b) the V-notch blunted by a circular damaged zone.

2. FFM coupled criterion for brittle materials

Consider the geometry is depicted in Figure 2(a). The failure prediction is based on the coupled criterion (Leguillon, 2002; Martin and Leguillon, 2004; Cornetti et al., 2006; Yosibash et al., 2006; Sapora et al., 2013; Weissgraeber et al., 2016). Its starting point is an energy balance (written in 2D omitting the specimen thickness)

$$\Delta \mathcal{W}^{\mathrm{P}} + \Delta \mathcal{W}^{\mathrm{K}} + \mathcal{G}_{\mathrm{c}} l = 0 \tag{2}$$

where $\Delta \mathcal{W}^{\mathrm{P}}$ and $\Delta \mathcal{W}^{\mathrm{K}}$ are respectively the change in potential energy and in kinetic energy between an uncracked state and a cracked one embedding a crack of length l, under a constant loading. The last term is the energy consumed to create such a crack, $\mathcal{G}_{\mathrm{c}}$ is the material toughness. As the initial loading is quasi-static then (2) becomes

$$-\Delta \mathcal{W}^{\mathrm{P}} \geq \mathcal{G}_{\mathrm{c}} l \tag{3}$$

If the crack length l at initiation is small compared to the dimensions of the structure (small compared to the notch depth in Figure 1 for instance), the problem can be described using matched asymptotic expansions. In the outer expansion, or far field, the displacements are given by

$$\underline{U}^{l}(x_1, x_2) = \underline{U}(x_1, x_2, l) = \underline{U}^{0}(x_1, x_2) + h_1(l)\underline{U}^{1}(x_1, x_2) + \ldots \text{ with } h_1(l) \to 0 \text{ as } l \to 0 \tag{4}$$

Here, $\underline{U}$ also noted $\underline{U}^l$ is the actual solution which depends on l. The leading term $\underline{U}^0$ is solution to the unperturbed problem (i.e. without crack, $l = 0$) and the following terms are small compared to that one. Such an expansion is valid throughout the entire structure except in a vicinity of the notch root where there is a short crack that is not taken into account by the successive terms $\underline{U}^0$, $\underline{U}^1$,… of the outer expansion. They are all settled on the unperturbed domain ($l = 0$, Figure 2a). The problem for $\underline{U}^1$ can be found in Leguillon (1989, 2011) and in Section 5, but it plays a minor role in the present analysis.

The inner expansion, or inner field, refers to a more detailed solution in the localized domain around the notch root. It is based on a zoom in by considering the stretched variables $y_i = x_i / l$

$$\begin{aligned}\underline{U}(x_1, x_2, l) &= \underline{U}(ly_1, ly_2, l) \\ &= H_0(l)\underline{V}^0(y_1, y_2) + H_1(l)\underline{V}^1(y_1, y_2) + \ldots \text{ with } \frac{H_1(l)}{H_0(l)} \to 0 \text{ as } l \to 0\end{aligned} \tag{5}$$

As $l \to 0$, the stretched dimensionless crack length is equal to 1 and the space spanned by (y_1, y_2) becomes unbounded. The matching conditions impose to the far field to coincide with the inner field in an intermediate region located close to the v-notch root in the outer domain and far from it in the inner domain (Van Dyke, 1964). The leading term of the behavior close to the v-notch in the outer domain is described by the Williams expansion (1), this leads to the matching conditions

$$H_0(l) = 1 \; ; \; \underline{V}^0(y_1, y_2) = \underline{R} \; ; \; H_1(l) = k \; l^\lambda \; ; \; \underline{V}^1(y_1, y_2) \cong \rho^\lambda \underline{u}(\theta) \text{ with } \rho = \frac{r}{l} \tag{6}$$

where the symbol $\cong$ means “behaves like at infinity” (i.e. as $\rho \to \infty$, that is far from the notch root in the inner domain). Using a superposition principle

$$\underline{V}^1(y_1 y_2) = \rho^\lambda \underline{u}(\theta) + \hat{\underline{V}}^1(y_1 y_2) \tag{7}$$

it is shown that $\hat{\underline{V}}^1$ and then $\underline{V}^1$ are solutions to well-posed problems. Indeed, existence and uniqueness of $\hat{\underline{V}}^1$ derives from the Lax-Milgram theorem within unbounded domains, in

particular $\underline{\hat{V}}^1$ has a finite energy. Then, existence and uniqueness of $\underline{V}^1$ follows even if its energy is unbounded. Finally, the inner expansion takes the form

$$\underline{U}(x_1, x_2, l) = \underline{U}(ly_1, ly_2, l) = \underline{R} + k\ l^{\lambda}\underline{V}^1(y_1, y_2) + \ldots \tag{8}$$

The change in potential energy due to the onset of the crack can be expanded as (Leguillon, 1989)

$$-\Delta \mathcal{W}^{\mathrm{P}} = A\ k^2 l^{2\lambda} + \ldots \tag{9}$$

where the scaling coefficient A (MPa^{-1}) is positive and depends only on the local geometry, i.e. the crack direction, not on its actual length. See Appendix 2 for the details of its computation. For example the coefficient A as a function of the opening angle ω is given in Figure 5.

Then the energy condition for the nucleation of the crack is

$$A\ k^2 l^{2\lambda - 1} \geq \mathcal{G}_{\mathrm{c}} \tag{10}$$

Since $2\lambda - 1$ is positive, the inequality (10) gives a lower bound for the admissible crack lengths l. This bound is even higher when the load (through k) is low. Clearly, if $\lambda > 0.5$ (i.e. except for a crack), if fracture occurs for a finite load, i.e. for a finite k, the length l cannot be infinitely small, there is a jump at initiation.

The stress condition states that the tensile stress σ must exceed the tensile strength σ_{c} all along the presupposed crack path (jump)

$$\sigma(r) \geq \sigma_{\mathrm{c}} \quad \text{for } 0 \leq r \leq l \tag{11}$$

With an appropriate normalization of the eigenvector $\underline{u}$ in (1) (i.e. $s_{\theta\theta}(0) = 1$, where $s_{\theta\theta}$ is the ortho-radial component of $\underline{\underline{s}}$ and where $\theta = 0$ corresponds to the bisector of the solid angle), using the Williams expansion (1) leads to

$$k\, r^{\lambda-1} \geq \sigma_c \quad \text{for } 0 \leq r \leq l \quad \Leftrightarrow \quad k\, l^{\lambda-1} \geq \sigma_c \tag{12}$$

The exponent $\lambda - 1$ is negative and (12) gives an upper bound of the admissible crack lengths l. It is small when the load is low. The compatibility between the two inequalities (10) and (12) is achieved by increasing the load. It leads to defining the crack length l_0 and the critical value of the GSIF k_c at initiation along the bisector (for symmetry reasons)

$$l_0 = \frac{G_c}{A}\frac{1}{\sigma_c^2} \;;\; k \geq k_c = \left(\frac{G_c}{A}\right)^{1-\lambda} \sigma_c^{2\lambda-1} \tag{13}$$

This criterion coincides with the classical Griffith criterion for a crack ($\omega = 0$, $\lambda = 0.5$) and with the tensile strength condition for a straight edge ($\omega = \pi$, $\lambda = 1$). Between the two, it evolves continuously from one to the other. A good agreement with experiments was found in many different cases (e.g. (Leguillon, 2002; Yosibash et al., 2006), see also the review paper by Weissgraeber et al. (2016)).

3. The damage model – Part I: the bounded stress field

Since the pioneering work of Kachanov (1958, 1986) (Lemaitre and Chaboche, 1985), it is usual in elasticity to describe damage by a local decrease of the material stiffness. In case of a singular point, the strain tensor tends to infinity when approaching this point. Thus, on one hand the Young modulus must decrease to zero so the stresses remain bounded. On the other hand, the Young modulus must tend to the material physical value at a given distance of the singular point. To this aim, we assume there exists a circular damaged area of radius d encompassing the notch root (Figure 2(b)), in which the Young modulus E' within this area follows a power law in terms of r (so that $E' \to 0$ as $r \to 0$) (Leguillon, 2008):

$$E' = E\left(\frac{r}{d}\right)^{\beta} \quad \text{for } r \leq d, \text{ with } \beta \geq 0 \;;\; E' = E \text{ otherwise} \tag{14}$$

where E is the Young modulus of the bulk material.

Obviously, such a damage law (14) is applicable only in the vicinity of elastic singular points. The circular damage zone assumption may be reconsidered in a future research. It is a limiting assumption whereas, for instance, the Von Mises stress iso-curves of the singular field (1) are

not circles around the notch root. Indeed, this simplifying assumption allows entering into the theory of singularities based on the separation of variables r and θ, and it leads to tractable analytical expressions. It is likely to be acceptable provided the damaged zone is small compared to the dimensions of the structure, as can be expected being only interested in the initiation step, not in the forthcoming crack growth. Moreover it is not completely unrealistic, such circular damaged area can be observed in some numerical simulations at the very beginning onset of damage (Moes et al., 2011). Otherwise, one would have to consider damaged zone shapes defined by an equation like $r(\theta) = \text{constant}$ and would make use of full finite elements (FE) computations.

A classical damage variable δ can be linked although it plays no direct role in the present analysis

$$E' = (1-\delta)E \quad \text{and then} \quad \delta(r) = 1 - \left(\frac{r}{d}\right)^{\beta}$$

Note that the damaged zone radius is not yet determined and will be addressed in the next section. According to the Hooke's law and in view of (14), within the damaged zone the elastic solution can be written as

$$\begin{cases} \underline{U}(r,\theta) = \underline{C} + k'\, r^{\xi}\, \underline{u}'(\theta) + \dots \\ \underline{\underline{\varepsilon}}(r,\theta) = k'\, r^{\xi-1}\, \underline{\underline{e}}'(\theta) + \dots \\ \underline{\underline{\sigma}}(r,\theta) = k'\, r^{\xi+\beta-1}\, \underline{\underline{s}}'(\theta) + \dots \end{cases} \tag{15}$$

The exponent ξ and the associated angular eigen-function $\underline{u}'$ are now solution to the following eigenvalue problem (see Appendix 1 for the definition of the operators **A**, **B** and **C**)

$$\left[-\xi(\xi+\beta)\mathbf{A} + \xi\mathbf{B} - (\xi+\beta)\mathbf{B}^{\mathrm{T}} + \mathbf{C}\right]\underline{u}' = 0 \tag{16}$$

that can be rewritten using the change of unknown exponent $\alpha = \xi + \beta/2$ (Apel et al., 2002)

$$\left[-\alpha^2\mathbf{A}+\alpha(\mathbf{B}-\mathbf{B}^{\mathrm{T}})+\mathbf{D}(\beta)\right]\underline{u}'=0 \quad \text{with } \mathbf{D}(\beta)=\mathbf{C}+\frac{\beta^2}{4}\mathbf{A}-\frac{\beta}{2}(\mathbf{B}+\mathbf{B}^{\mathrm{T}}) \tag{17}$$

The operator **D** is still symmetric, thus the solutions to (17) enjoy the same properties as that of (A1.1) (see Appendix 1). In particular, if the pair $(\alpha,\underline{u}')$ is a solution, then the dual $(-\alpha,\underline{u}'^{-})$ is also a solution. In other words, the dual to $(\xi,\underline{u}')$ is $(-\xi-\beta,\underline{u}'^{-})$.

According to (17), the exponent α is a function of β and the stress tensor in (15) becomes

$$\underline{\underline{\sigma}}(r,\theta)=k'\,r^{\alpha+\beta/2-1}\underline{\underline{s}}'(\theta)+... \tag{18}$$

This stress field remains bounded as $r\to 0$ if

$$\alpha(\beta)+\beta/2-1=0 \tag{19}$$

where the dependence of α on β has been highlighted. Note that for positive values of the left hand side member of (19) the stress field would vanish at the corner but there is no physical need for that. Thus, according to this remark, the Williams expansion takes the final form

$$\begin{cases}\underline{U}(r,\theta)=\underline{C}+k'\,r^{1-\beta}\underline{u}'(\theta)+...\\ \underline{\underline{\varepsilon}}(r,\theta)=k'\,r^{-\beta}\underline{\underline{e}}'(\theta)+...\\ \underline{\underline{\sigma}}(r,\theta)=k'\,\underline{\underline{s}}'(\theta)+...\end{cases} \tag{20}$$

The strain field remains singular, whereas the stress field is bounded. A similar feature is met in the HRR solution for power hardening materials (Hutchinson, 1968; Rice and Rosengren, 1968) where, even if the two fields remain singular, the strain one is much more singular than the stress one.

This result is illustrated in Figure 3 where the exponent β is plotted as functions of the opening angle ω.

An important feature must be pointed out. When $\omega=\pi$ (straight edge) there is no longer any singularity ($\lambda=1$ in (1)) and the stress field remains bounded and constant in the vicinity of

any point of the boundary (tensile stress parallel to the boundary), as a consequence $\beta = 0$ in (14), then $E' = E$ and the damaged zone disappears. Thus, according to this damage law, there is no diffuse damage. Damage can only occur in areas of high stress concentration. This damage law seems particularly appropriate to quasi-brittle materials.

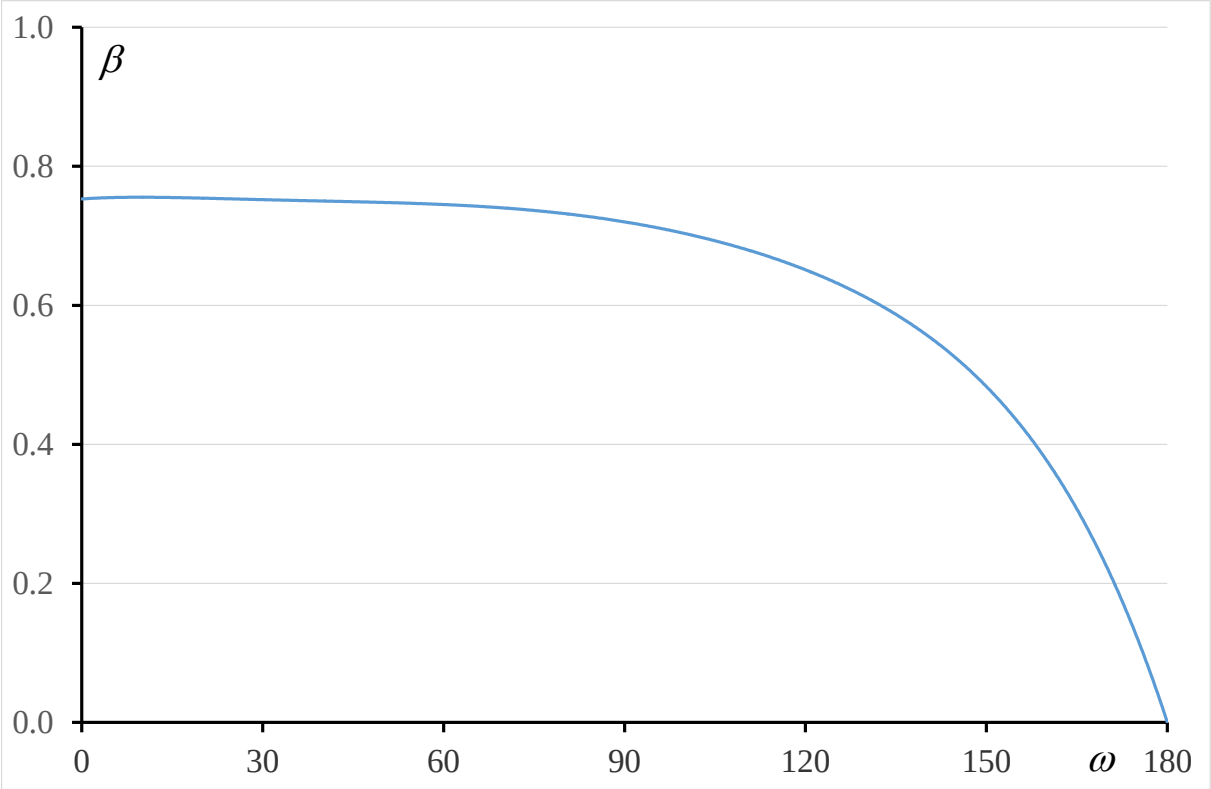

Figure 3. The exponents β ensuring a bounded stress field at the V-notch as a function of the opening angle ω (deg.).

In Figure 4, the tensile stress along the bisector of the solid angle in presence of a damage zone of radius 1 mm is compared to the singular tensile stress (1) for an opening angle $\omega = \pi / 2$ ($\lambda = 0.545$, $\beta = 0.72$). It is clearly bounded and the small drop that can be seen near $r = 0$ is only a small inaccuracy in the FE calculation due to the close proximity of the two traction free faces of the notch. It is slightly varying in the damage zone and (20) represents the asymptotic trend as approaching the notch tip, i.e. at a small distance compared to the damage zone radius. Both numerical approach (Figure 3) and (20) are in a good agreement in the vicinity of the corner as shown in (Leguillon, 2008). The computation was carried out on a large (compared to the unit radius of the damaged zone) circular domain with a 90 deg. notch, prescribing the singular mode $r^{\lambda}\underline{u}(\theta)$ on the outer boundary which proves useful in the

determination of the term of the inner expansions (see the superposition principle and Eqn. (6)). The resulting stress field is dimensionless.

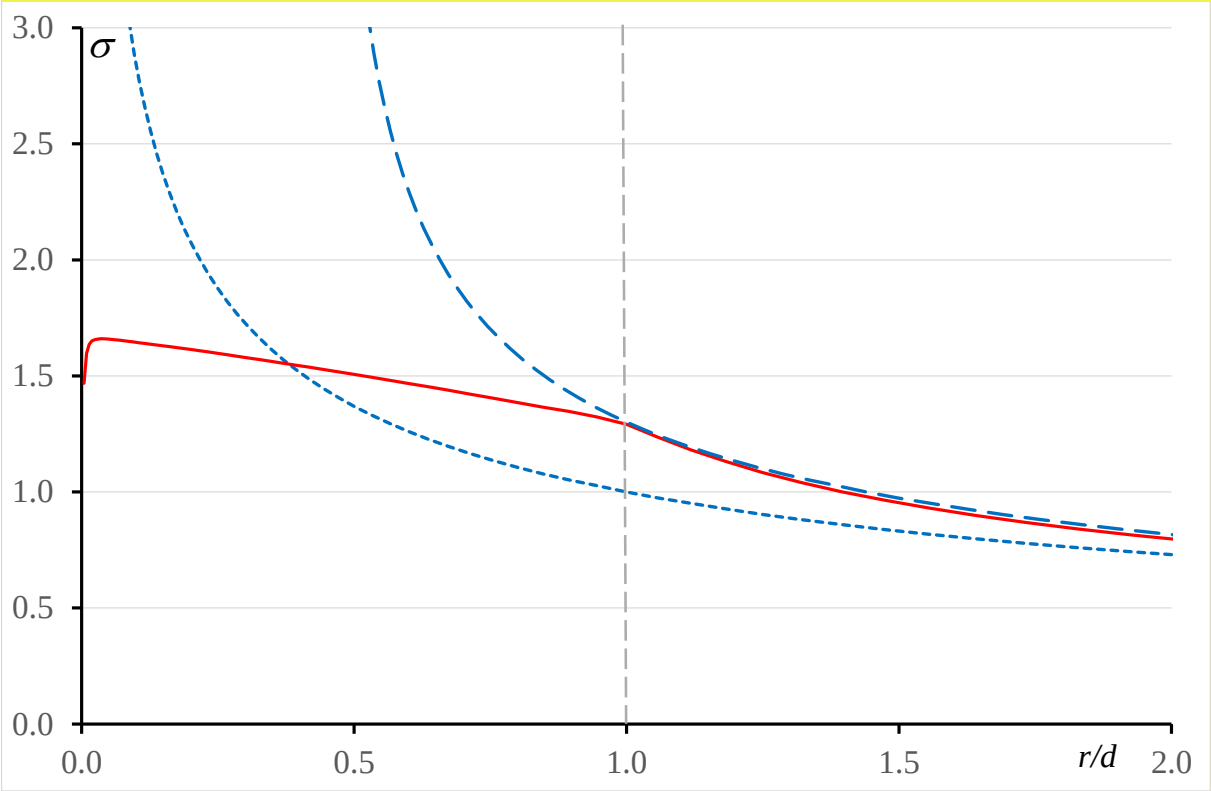

Figure 4. The dimensionless tensile stress σ along the bisector of the angle for $\omega = \pi / 2$ as a function of the dimensionless distance r / d to the notch root ($\sigma_{\theta\theta} \equiv \sigma_{22} \equiv \sigma$); (i) with a damage zone of radius 1 (red solid line), (ii) without damage zone (singular behavior) (blue dotted line), (iii) the same singular curve shifted by 0.44 on the right (blue dashed line).

By analogy with a suggestion of Rice (1968) studying the effect of a small scale yielding plastic zone at the tip of a crack, the tensile stress out of the damaged zone appeared to be quite similar to the singular stress curve shifted by 0.44 on the right (Figure 4). It means that away from the notch root (i.e. out of the damage zone), the influence of the damaged zone on the far field is equivalent to that of a virtual crack of length $\bar{d} = 0.44\, d$. It is numerically checked that it is independent of the opening angle ω .

4. The damage model – Part II: determination of the size of the damage zone (*d*)

Assuming that the damage zone is small compared to the dimensions of the structure, the elastic solution can be again described using matched asymptotic expansions with respect to d . The outer expansion can be written

$$\underline{U}^{d}(x_1,x_2)=\underline{U}(x_1,x_2,d)=\underline{U}^{0}(x_1,x_2)+f_1(d)\underline{U}^{1}(x_1,x_2)+\ldots \text{ with } f_1(d)\to 0 \text{ as } d\to 0 \quad (21)$$

Here, $\underline{U}$ also noted $\underline{U}^{d}$ is the actual solution which depends on the radius d of the damaged zone. The leading term $\underline{U}^{0}$ is solution to the unperturbed problem (i.e. without damaged area, $d=0$) and the following terms are small compared to that one. Note that the functions $\underline{U}^{0}$ and $\underline{U}^{1}$ in (21) are the same as in (4), the difference lies in the weight factors $h_1(l)$ and $f_1(d)$.

Such an expansion (21) is valid throughout the entire structure except in a vicinity of the notch root, i.e. in a vicinity of the damaged zone.

The inner expansion, or inner field, refers to a more detailed solution in a localized domain around the notch root. It is based on a zoom in $z_i=x_i/d$

$$\begin{aligned}\underline{U}(x_1,x_2,d)&=\underline{U}(dz_1,dz_2,d)\\&=F_0(d)\underline{W}^{0}(z_1,z_2)+F_1(d)\underline{W}^{1}(z_1,z_2)+\ldots \text{ with } \frac{F_1(d)}{F_0(d)}\to 0 \text{ as } d\to 0\end{aligned} \quad (22)$$

As $d\to 0$, the dimensionless stretched radius of the damage area is 1 and again the space spanned by (z_1,z_2) becomes unbounded. The matching rules are the same as in Section 3, again the leading term of the behavior close to the v-notch in the outer domain is described by the Williams expansion (1). This leads to the matching conditions

$$F_0(d)=1\ ;\ \underline{W}^{0}(z_1,z_2)=\underline{R}\ ;\ F_1(d)=k\ d^{\lambda}\ ;\ \underline{W}^{1}(z_1,z_2)\cong\zeta^{\lambda}\underline{u}(\theta) \text{ with } \zeta=\frac{r}{d} \quad (23)$$

where the symbol $\cong$ means “behaves like at infinity” (i.e. as $\zeta\to\infty$, that is far from the notch root in the inner domain). Using a similar superposition principle as in Section 2

$$\underline{W}^{1}(z_1,z_2)=\zeta^{\lambda}\underline{u}(\theta)+\hat{\underline{W}}^{1}(z_1,z_2) \quad (24)$$

In Appendix 3 we show that $\underline{\hat{W}}^1$ and then $\underline{W}^1$ are solutions to well-posed problems, and detail the algorithm for the computation of $\underline{\hat{W}}^1$.

The inner expansion takes the form

$$\begin{aligned} \underline{U}(x_1, x_2, d) &= \underline{U}(dz_1, dz_2, d) \\ &= \underline{R} + k\ d^{\lambda}\underline{W}^1(z_1, z_2) + \ldots \end{aligned} \tag{25}$$

The energy balance now refers to the energy $\Delta\mathcal{W}^{\mathrm{D}}$ required to damage the specified zone

$$\Delta\mathcal{W}^{\mathrm{P}} + \Delta\mathcal{W}^{\mathrm{K}} + \Delta\mathcal{W}^{\mathrm{D}} = 0 \tag{26}$$

Following Leguillon (1989), the change in potential energy due to the creation and evolution of the damage zone can be expressed as

$$-\Delta\mathcal{W}^{\mathrm{P}} = L\ k^2 d^{2\lambda} + \ldots \tag{27}$$

The coefficient L (MPa^{-1}) is positive and depends only on the local geometry, i.e. on the opening angle ω and the shape of the damaged zone (but not its size) it can be calculated using a path independent integral (see Appendix 2). In Figure 5, L decreases to 0 as $\omega \to \pi$. This is a consequence of the choice of the damage law, when $\omega = \pi$ the damaged zone disappears (see Section 3).

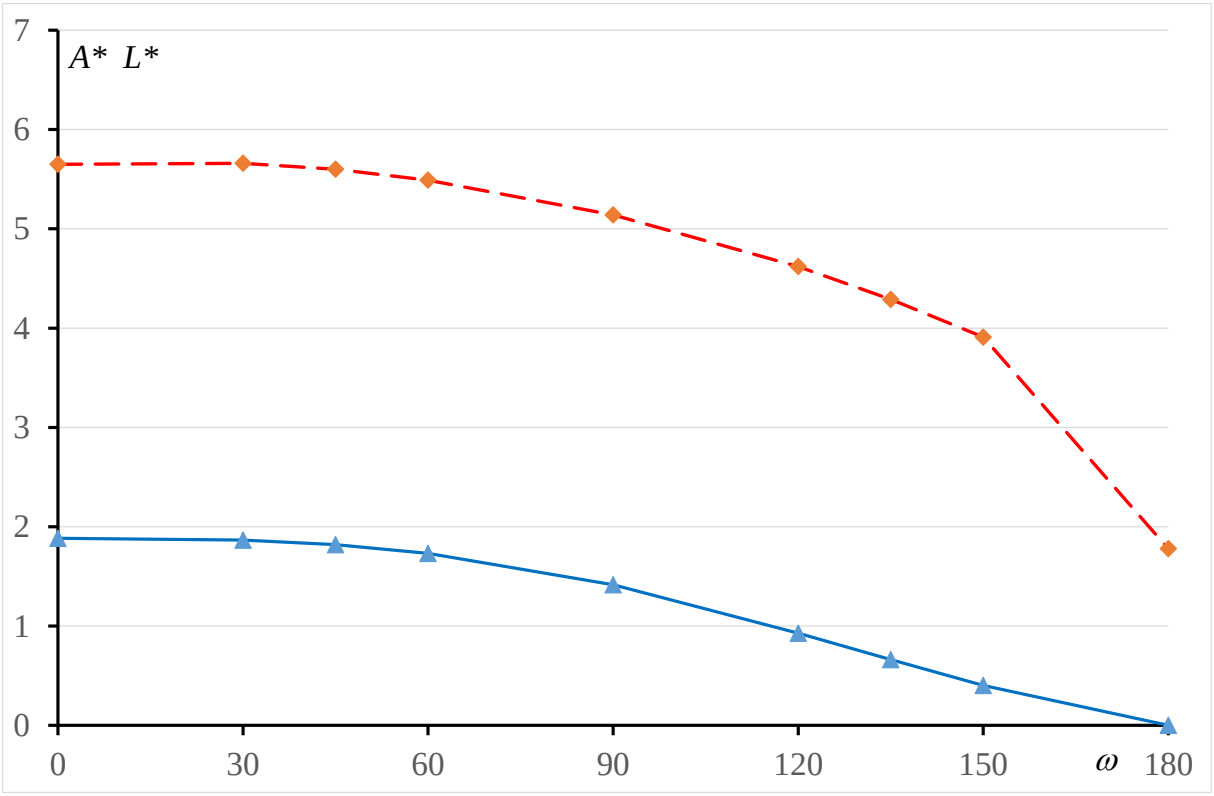

Figure 5. The dimensionless scaling coefficients $A^* = EA$ (red dashed line) (Eqn. (10)) and $L^* = EL$ (blue solid line) (Eqn. (29)) as functions of the opening angle ω (deg.) for $\nu = 0.3$.

Note that the curves in Figure 5 could also depend on the Poisson ratio but it is numerically checked that they almost not vary in a wide range from $\nu = 0.1$ to 0.4. They are plotted here for $\nu = 0.3$.

The dissipation energy is manifested in the change in Young's modulus (i.e. damages the material). We compute it herein, when a damage zone of a radius d is created. This dissipation energy is proportional with the relative change in Young's modulus ΔE and of course proportional with the damaged area

$$\Delta \boldsymbol{w}^{\mathrm{D}} = D_{\mathrm{c}} \int_{-\pi+\omega/2}^{\pi-\omega/2} \int_{0}^{d} \frac{\Delta E}{E} \, r \mathrm{d}r \mathrm{d}\theta \tag{28}$$

Where we denote the constant of linear proportionality by D_c (MPa), assuming it to be a material parameter. The physical interpretation of D_c is given in Appendix 4 and we elaborate on it in Section 5. Recalling (14), we obtain that

$$\frac{\Delta E}{E} = \frac{E - E'}{E} = \frac{E - E\left(\frac{r}{d}\right)^{\beta}}{E} = 1 - \left(\frac{r}{d}\right)^{\beta} \tag{29}$$

Inserting (29) in (28) and integrating, we obtain:

$$\Delta \boldsymbol{W}^{\mathrm{D}} = \frac{\beta(2\pi - \omega)}{2(\beta + 2)} D_{\mathrm{c}} d^{2} \tag{30}$$

Recall that β defined in (19) determines the exponent governing the change of E so that $\underline{\underline{\sigma}}$ remains bounded as $r \to 0$. Inserting (30) and (28) in (27), then under a quasi-static loading, the energy condition to ensure the existence of a damage zone of dimension *d*

$$L k^{2} d^{2\lambda - 2} \geq \frac{\beta(2\pi - \omega)}{2(\beta + 2)} D_{\mathrm{c}} \tag{31}$$

The exponent 2λ-2 being negative, (31) provides an upper bound for the admissible damage zone size as a function of the external load (through k)

$$d^{2(1-\lambda)} = \frac{L k^{2} 2(\beta + 2)}{D_{\mathrm{c}} \beta(2\pi - \omega)} \tag{32}$$

In this case there is no discontinuity (no jump), d is directly related to the applied load through k and stably grows from 0 as k increases. Unlike the crack initiation, this stability was expected and it suits well a damage mechanism.

According to the remark following Figure 4, a good approximation of the tensile stress σ, i.e. the hoop stress, of the actual solution along the boundary of the damaged zone on the bisector of the solid angle ($\theta = 0$) is

$$\sigma(d, 0) = k\left(ad\right)^{\lambda - 1} \text{ with } ad = d - \overline{d} \tag{33}$$

where it is recalled that $\bar{d} = 0.44d$ is the virtual offset of the notch root and then $a = 0.56$ (Section 3). Inserting (32) into (33) shows that the stress is independent of the applied load, i.e. independent of k

$$\sigma(d,0) \approx a^{\lambda-1}\sqrt{\frac{\beta(2\pi-\omega)}{2(\beta+2)}\frac{D_c}{L}} \tag{34}$$

Moreover, it is numerically checked that this relationship holds true whatever the direction θ under the generalized form

$$\sigma(d,\theta) \approx a^{\lambda-1}\sqrt{\frac{\beta(2\pi-\omega)}{2(\beta+2)}\frac{D_c}{L}s_{\theta\theta}(\theta)} \tag{35}$$

Indeed, the functions $s_{\theta\theta}$ in (1) and $s'_{\theta\theta}$ in (20) coincide, this is not true for the other components.

The boundary of the damaged zone acts somewhat like a threshold in the stress field, it can be defined either by its radius (32) or by (34). As the tensile stress is increasing when approaching the notch root, if the tensire stress is smaller than the value in (34) and (35) then it is out of the damage zone. This may suggest something like the yield stress in an elastoplastic behavior, however there is a drawback: this threshold seems to depend on the opening angle through λ and β in the two above relationships, thus it cannot be considered as a material parameter. However, it is observed in the numerical application (Section 7) that it remains almost constant in a wide range of opening angles ($\omega < 120$ deg.).

5. Identification of D_c

The scaling coefficient D_c in (28) is a material parameter. We propose in this section a method for its identification from an appropriate experiment. Let us suppose that, using a full field measurement and a Digital Image Correlation (DIC) system (see the review paper by Hild and Roux (2006)), we are able to obtain a reliable displacement field $\underline{U}^{DIC}$ in a bending

test for instance, this measured field is $\underline{U}^d$ in (21). Next, it is possible to derive from this known displacement field the size d of the damage zone and then the parameter D_c.

We refer to (Leguillon, 2011) for most of the results in this section. Let us make explicit the second term of the outer expansion (21)

$$f_1(d) = k\tilde{L}d^{2\lambda} \quad \text{with} \quad \tilde{L} = \frac{L}{\Psi(\zeta^{-\lambda}\underline{u}^-, \zeta^{\lambda}\underline{u})} = \frac{\Psi(\hat{\underline{W}}^1, \zeta^{\lambda}\underline{u})}{\Psi(\zeta^{-\lambda}\underline{u}^-, \zeta^{\lambda}\underline{u})} \tag{36}$$

where $\tilde{L}$ is dimensionless. It is the GSIF associated with the dual mode $\zeta^{-\lambda}\underline{u}^-(\theta)$ in $\hat{\underline{W}}^1$ or $\underline{W}^1$ (see Eqn. (24)) in the analogue to a Williams' expansion of $\hat{\underline{W}}^1$ at infinity. This is a consequence of the matching conditions.

Again, a superposition principle

$$\underline{U}^1(x_1, x_2) = r^{-\lambda}\underline{u}^-(\theta) + \hat{\underline{U}}^1(x_1, x_2) \tag{37}$$

can be invoked to show that $\hat{\underline{U}}^1$ is solution to a well-posed problem with a finite energy (belonging to a usual Sobolev space), and so is $\underline{U}^1$ but obviously now with a non-finite energy. Using this decomposition, the outer expansion (21) can be written

$$\begin{aligned} &\underline{U}^{\mathrm{DIC}}(x_1, x_2) = \underline{U}^0(x_1, x_2) + k\tilde{L}d^{2\lambda}\left[r^{-\lambda}\underline{u}^-(\theta) + \hat{\underline{U}}^1(x_1, x_2)\right] + f_2(d)\underline{U}^2(x_1, x_2) + \ldots \\ &\text{with } \frac{f_2(d)}{d^{2\lambda}} \to 0 \text{ as } d \to 0 \end{aligned} \tag{38}$$

The term $k\tilde{L}d^{2\lambda}$ in (38) appears to be the GSIF k^- (MPa mm$^{1+\lambda}$) of the dual (super singular) mode $r^{-\lambda}\underline{u}^-(\theta)$, or at least the leading term in an expansion of k^-. Analogously to k in (1), it can be extracted from $\underline{U}^d$ using the Ψ integral (Appendix 1)

$$k^- = k\tilde{L}d^{2\lambda} = \frac{\Psi(\underline{U}^{\mathrm{DIC}}, r^{\lambda}\underline{u})}{\Psi(r^{-\lambda}\underline{u}^-, r^{\lambda}\underline{u})} \tag{39}$$

Having k^-, k and $\tilde{L}$, (39) allows to determine d

$$d = \left(\frac{k^-}{k\tilde{L}} \right)^{\frac{1}{2\lambda}} \tag{40}$$

And consequently by (32), one may finally determine D_c

$$D_c = \frac{2(\beta + 2)Lk^2}{\beta(2\pi - \omega)d^{2(1-\lambda)}} \tag{41}$$

Subsection 7.5 addresses also the determination of d and the identification of D_c by a FE simulation instead of a full-field measurement.

6. Coupling the damage zone model with the FFM coupled criterion

The damage zone grows with the load, i.e. with *k*. Therefore it pre-exists to the virtual crack which is considered only beyond a threshold load (see Eqn. (13)). Thus, the energy criterion for the failure initiation due to the crack must consider a change in potential energy due to the uncracked and the cracked states of the damaged structure. Reconsidering the energy balance (2) it is now stated as (the prime denotes variable quantities due to damage)

$$\Delta \mathcal{W}^{\mathrm{P}} + \Delta \mathcal{W}^{\mathrm{K}} + \int_0^l G_c'(r)\mathrm{d}r = 0 \quad \Rightarrow \quad -\Delta \mathcal{W}^{\mathrm{P}} \geq \int_0^l G_c'(r)\mathrm{d}r \tag{42}$$

This form of the fracture energy allows to consider a variable toughness as it likely occurs in the damaged zone (Leguillon et al., 2016) (see Section 7.3). We suppose that at a distance r of the notch root the damage characterized by E' is such that $G_c'(r)\mathrm{d}r$ is the energy required to create a short crack with length $\mathrm{d}r$. If $r \geq d$ then $G_c'(r) = \mathcal{G}_c$. The function $G_c'(r)$ is somehow a "local" toughness varying or not with the level of damage. It is an artifact because this function cannot be experimentally determined. It would be necessary to introduce a crack with its tip in the vicinity of the point under consideration but which does not modify the surrounding properties (damage) when it is loaded. One can only assume that this local toughness varies with the damage and then verify that it gives consistent results with

experimental measures when available, as in the case of oxidized polymers (Leguillon et al., 2016). See the discussion in Section 7.1.

If the radius of the damage zone and the virtual crack length are of the same order of magnitude (i.e. $d \approx l$, to be a posteriori checked) the two small parameters tend to 0 simultaneously and the outer expansion (21) is almost unchanged except in the weight term $g_1(d)$

$$\begin{aligned} &\underline{U}^{dl}(x_1,x_2) = \underline{U}(x_1,x_2,d,l) = \underline{U}^0(x_1,x_2) + g_1(d)\underline{U}^1(x_1,x_2) + \dots \\ &\text{with } g_1(d) \to 0 \text{ as } d \to 0 \end{aligned} \tag{43}$$

But the inner expansion describing the crack onset must be rewritten to account for both the damage zone and the crack length (note that $d > 0$ since a damage zone starts to grow monotonically with *k*)

$$\begin{aligned} \underline{U}(x_1,x_2,d,l) &= \underline{U}(dz_1,dz_2,d,d\mu) \\ &= \underline{R} + k\ d^{\lambda}\underline{W}^1(z_1,z_2,\mu) + \dots \\ &= \underline{R} + k\ d^{\lambda}\left[\zeta^{\lambda}\underline{u}(\theta) + \underline{\hat{W}}^1(z_1,z_2,\mu)\right] + \dots \text{ with } \mu = \frac{l}{d} \end{aligned} \tag{44}$$

The additional conditions fulfilled by $\underline{W}^1$ and $\underline{\hat{W}}^1$ on the two crack faces can be found in Appendix 3.

The function $\underline{W}^1$ depends now on l through μ. Note that the function $\underline{W}^1(z_1,z_2)$ in (22) is the present $\underline{W}^1(z_1,z_2,0)$. The change in potential energy takes the special form (Leguillon et al., 2007)

$$-\Delta \mathcal{W}^{\mathrm{P}} = k^2 d^{2\lambda}\left[B(\mu) - B(0)\right] + \dots \tag{45}$$

The term $B(\mu)$ and $B(0)$ correspond respectively to the damaged cracked state and the damaged uncracked one, again they can be calculated using a path independent integral (see Appendix 2). For an uncracked configuration, following section 4, we identify that $B(0) \equiv L$. Substituting (45) in (42), the energy condition can be formulated as follows

$$k^2 d^{2\lambda}\left[B(\mu)-L\right] \geq \int_0^l G_c'(r)\mathrm{d}r \tag{46}$$

Since the crack length can be smaller or larger than the radius of the damaged zone, the stress tensor acting along the bisector of the solid angle ($\theta = 0$) is no longer described by an asymptotic expansion as in (1) or (15). Let us denote σ the tensile component along the bisector and $\tilde{\sigma}$ the same tensile component in the inner expansion coordinates. Because of the change of space variables $y_i = x_i / d$, according to (44), $\sigma = k\, d^{\lambda} \times 1/d\ \ \tilde{\sigma} = k\, d^{\lambda-1}\tilde{\sigma}$, where $\tilde{\sigma}$ is dimensionless and then the stress condition can be written

$$\begin{aligned} \sigma(r) \geq \sigma_c'(r) \ \text{ for } 0 \leq r \leq l \ \ &\Rightarrow \ \ k\, d^{\lambda-1}\tilde{\sigma}(\rho) \geq \sigma_c'(\rho) \ \text{ for } 0 \leq \rho \leq \mu \\ &\Rightarrow \ \ k\, d^{\lambda-1}\tilde{\sigma}(\mu) \geq \sigma_c'(\mu) \end{aligned} \tag{47}$$

Indeed, the stress condition of the (DEFINE CC) CC states that the tensile stress along the expected crack path prior to the crack onset must exceed the tensile strength. In the present case, this means that the expected crack path is located in the damage zone and may also exceed it. This explains that the stress condition must be applied within the inner domain where the damage zone is visible. In the classical case (Leguillon, 2002), it is usually applied in the outer domain because asymptotics are carried out with respect to the crack length and then prior to the crack onset there is no perturbation, inner and outer expansions are similar. Whereas, in the present case, the asymptotics are carried out with respect to the damage zone radius. The situation is somewhat similar to that of the blunted V-notch where asymptotics are carried out with respect to the root radius not with respect to the crack length (Leguillon and Yosibash, 2003).

Alike the toughness, the tensile strength likely changes in the damage zone and (47) holds true provided that $\sigma_c'(r)$ is constant or decreases as the damage increases (i.e. as E' decreases), which seems a reasonable assumption (Leguillon et al., 2016) (see Section 7.3). Combining (46) and (47) gives an equation for the unknown critical virtual crack length l_c as a function of d

$$\frac{1}{\tilde{\sigma}(\mu_c)^2}\left[\frac{B(\mu_c)-L}{\mu_c}\right]=\frac{1}{d}\frac{\bar{G}'_c(\mu_c)}{\sigma'_c(\mu_c)^2} \quad \text{with} \quad \bar{G}'_c(\mu_c)=\frac{1}{l_c}\int_0^{l_c} G'_c(r)\mathrm{d}r \quad \text{and} \quad l_c=\mu_c d \tag{48}$$

Here $\bar{G}'_c$ depends on d and μ_c through l_c. Substituting (48) into (46) leads to the condition for failure initiation

$$k \geq k_c^{\mathrm{dam}}=\left(\frac{\mu_c \bar{G}'_c(\mu_c)}{B(\mu_c)-L}\right)^{1-\lambda}\left(\frac{\sigma'_c(\mu_c)}{\tilde{\sigma}(\mu_c)}\right)^{2\lambda-1} \tag{49}$$

Note that the right hand side depends on k through μ_c which depends on d (48) which itself is a function of k (32), so (49) is an implicit equation.

Note that an alternative approach is to consider the total change in potential energy, denoted $\Delta \mathcal{W}^{\mathrm{T}}$, between the uncracked and undamaged state and the damaged and cracked one. Then the energy balance equation can be written

$$\Delta \mathcal{W}^{\mathrm{T}}+\Delta \mathcal{W}^{\mathrm{K}}+\Delta \mathcal{W}^{\mathrm{D}}+\int_0^l G'_c(r)\mathrm{d}r=0 \tag{50}$$

This leads to the inequality

$$-\Delta \mathcal{W}^{\mathrm{T}} \geq \int_0^l G'_c(r)\mathrm{d}r+\Delta \mathcal{W}^{\mathrm{D}}=\int_0^l G'_c(r)\mathrm{d}r+L\ k^2 d^{2\lambda} \tag{51}$$

From (2) and (51), we can already note that as expected, if $G'_c(r)$ is unchanged in the damage zone ($G'_c(r)=\mathcal{G}_c$), then the load triggering the crack onset will be larger in presence of the damage zone than in the brittle case, i.e. without damage. The damage zone "blunts" the notch (Leguillon and Yosibash, 2003; Picard et al., 2006; Carpinteri et al., 2012).
The total change in potential energy can be written

$$-\Delta \mathcal{W}^{\mathrm{T}}=k^2 d^{2\lambda} B(\mu)+\ldots \tag{52}$$

Then the energy balance (51) is the same as in (46)

$$k^2 d^{2\lambda}\left[B(\mu)-L\right] \geq \int_0^l G_c'(r)\mathrm{d}r$$

That leads to the final form (48) and (49) of the criterion.

7. Numerical results

• In a first step, the functions $\tilde{\sigma}(\mu)$ and $B(\mu)$ have to be tabulated for different values of ω (0, 30, 60, 90, 120, 150, 180 deg. for instance) by solving once and for all the inner problems which solution is $\underline{\hat{W}}^1(z_1, z_2, \mu)$ (see Eqn. (44)), varying μ from 0 to 2 by unbuttoning nodes (Appendix 3). Remember that $B(0) = L$.

• The second step consists in determining the critical load at failure, i.e. the critical value of the GSIF k. The non-linear equation resulting of (49) (the right hand side member depends on k)

$$k = \left(\frac{\mu \bar{G}_c'(\mu)}{B(\mu)-L}\right)^{1-\lambda}\left(\frac{\sigma_c'(\mu)}{\tilde{\sigma}(\mu)}\right)^{2\lambda-1} \tag{53}$$

is solved for k using an iterative Newton procedure. Within each iteration, for a given value of the iterate $k_{(n)}$, the non-linear equation

$$\frac{1}{\tilde{\sigma}(\mu)^2}\frac{B(\mu)-L}{\mu} = \frac{1}{d_{(n)}}\frac{\bar{G}_c'(\mu)}{\sigma_c'(\mu)^2} \tag{54}$$

is solved for μ again using an iterative Newton procedure, $d_{(n)}$ being calculated by (32)

$$d_{(n)} = \left(\frac{Lk_{(n)}^2 2(\beta+2)}{D_c \beta(2\pi-\omega)}\right)^{\frac{1}{2(1-\lambda)}} \tag{55}$$

There are two nested loops.

• The final step is to solve the outer problem (i.e. neglecting both the damage zone and the crack length) corresponding to an actual structural problem, then to compute the GSIF k (Appendix 1) and to compare this value to the critical one determined at the previous step.

Calculations are carried out for various V-notch opening angles $\omega =$ 0 to 150 deg. Typical value of graphite are used, $E = 9600$ MPa, $\nu = 0.3$, $\sigma_c = 25$ MPa, $\mathcal{G}_c =$ 0.14 MPa mm (in a first step constant values of the tensile strength and toughness are assumed). Calculations reveal to be sensitive to the scaling parameter D_c reflecting the tendency of the material to damage. It is empirically chosen $D_c = 0.096$ MPa ($D_c / E = 10^{-5}$) for having consistent results in the damaged zone size, it remains small compared to the dimensions of the structure.
A sensitivity analysis follows in Section 7.2. With these data, according to (34), the hoop stress $\sigma(d,0)$ on the bisector of the solid angle ($\theta = 0$) at the boundary of the damage zone slightly varies around 26.5 MPa for a wide range of opening angles ($\omega < 120$ deg.), $\sigma(d,0) =$ 26.2 MPa for $\omega = \pi / 2$ for instance. Then it starts to increase (indefinitely when $\omega \to \pi$).

7.1 *Variable opening, fixed* D_c, σ_c *and* G_c

In that case the damage has no influence on the fracture parameters and $G_c'(r) = \mathcal{G}_c$. Figure 6 shows the critical GSIF in the two cases: k_c^{dam} considering a damaged zone (49) compared to k_c without a damaged zone (13) (brittle material). One may notice that $k_c^{dam} > k_c$ and thus that the damage zone "blunts" the notch. At the limit as $\omega \to \pi$, $k_c = k_c^{dam} = \sigma_c =$ 25 MPa (keep in mind that $k = \sigma$ for $\omega = \pi$).

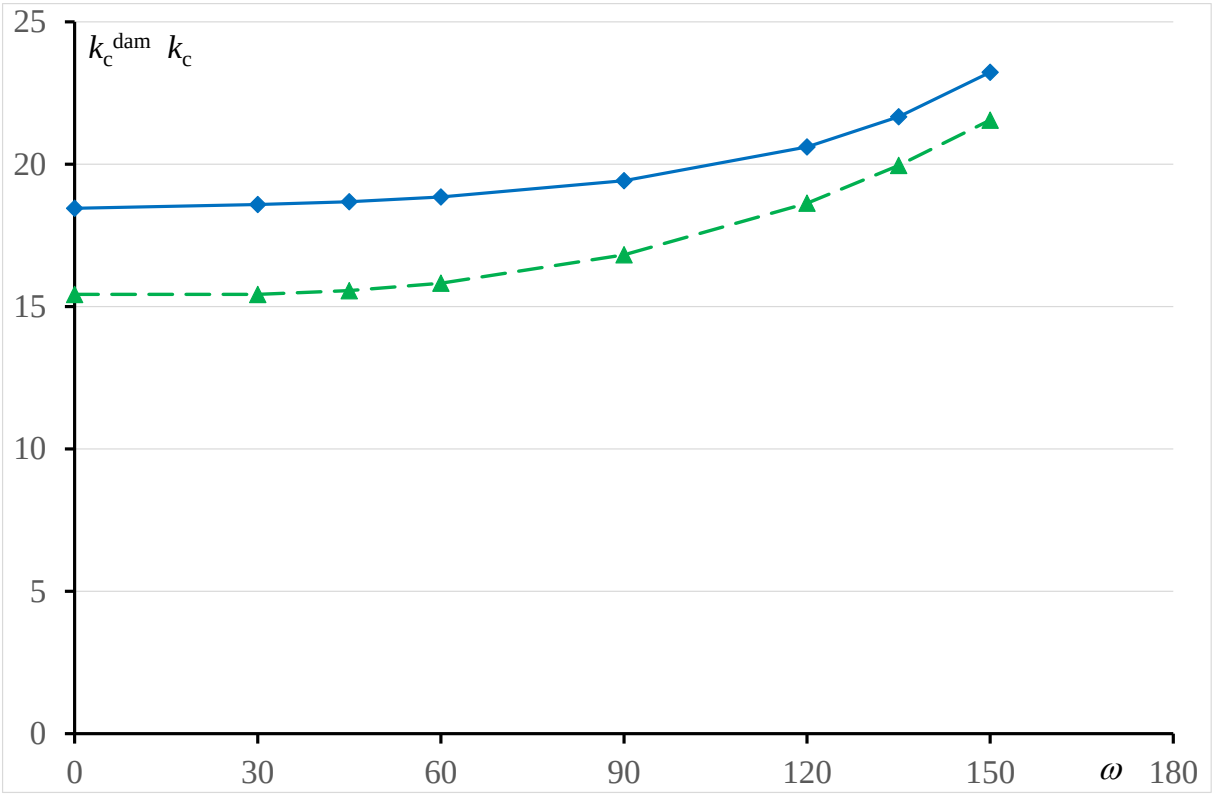

Figure 6. The critical GSIF's k_c^{dam} (49) with a damaged zone (blue solid line) and k_c (13) without damaged zone (green dashed line), as a function of the opening angle ω (deg.). Units of GSIF's (MPa mm$^{1-\lambda}$) are not specified because they vary with the opening angle ω.

On the one hand, from Figure 6 for $\omega = 0$ ($\lambda = 0.5$), the toughness $\mathcal{G}_c'$ of the quasi-brittle material can be compared to the toughness $\mathcal{G}_c$

$$\mathcal{G}_c' = \left(\frac{k_c^{dam}(\omega = 0)}{k_c(\omega = 0)} \right)^2 \mathcal{G}_c = \left(\frac{k_{Ic}'}{k_{Ic}} \right)^2 \mathcal{G}_c = 1.43\, \mathcal{G}_c \tag{56}$$

It is the material toughness that would be measured during a test on a quasi-brittle material damaging according to the law proposed in Section 3. It takes into account the two last terms in the energy balance (50) corresponding to two different sources of dissipation

$$\mathcal{G}_c' l = \Delta \mathcal{W}^D + \mathcal{G}_c l \tag{57}$$

Contrary, $\mathcal{G}_c$ cannot be measured, it is the toughness of a virtual equivalent material which does not damage, it is just used to allow a better understanding of the role of the damage zone by separating the two mechanisms, damage and crack onset.

On the other hand, the tensile strength can be identified for $\omega = \pi$ and gives $\sigma'_c = \sigma_c = 25$ MPa. Thus, by analogy with the case of a brittle material (Section 2), i.e. using the coupled criterion with the measured parameters, the critical GSIF is given by

$$k'_c = \left(\frac{\mathcal{G}'_c}{A} \right)^{1-\lambda} (\sigma'_c)^{2\lambda-1} \tag{58}$$

It is plotted in Figure 7 (red dashed line) and is very closed to k_c^{dam}.

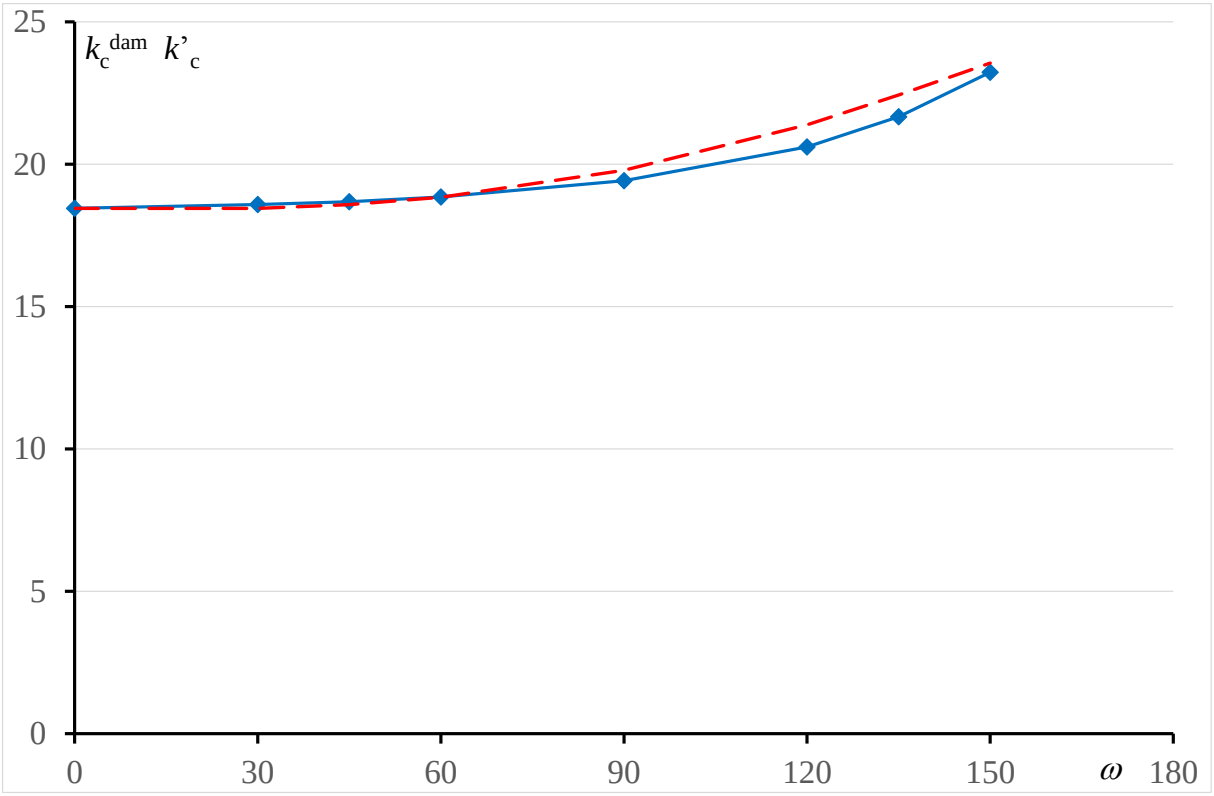

Figure 7. The critical GSIF k_c^{dam} (49) (blue solid line) compared to k'_c (58) obtained by applying the coupled criterion to the identified strength and toughness of the quasi-brittle material, as a function of the opening angle ω (deg.). Again, units of GSIF's (MPa mm$^{1-\lambda}$) are not specified because they vary with the opening angle ω.

This shows that the crack initiation at the root of a V-notch in a quasi-brittle material is still described by the coupled criterion, using the actual toughness as measured on a cracked

specimen. This is expected to greatly simplify the calculation algorithm as only $B(\mu)$ for ω = 0 must be tabulated to calculate $k_c^{dam}(\omega = 0)$ and then to identify $\mathcal{G}_{f_c}'$.

It could be emphasized that if $\mathcal{G}_{f_c}'$ is measured and if the damage law is known, then $\mathcal{G}_{f_c}$ can be determined using (56) and it is then possible to analyze the changes that could occur if the damage parameters vary as a function of an external phenomenon (e.g. temperature, moisture, oxidation ...).

Figure 8 shows the damage zone size d and the critical crack length l_c. The damage zone size tends to 0 as the opening ω approaches π because at the limit there is no longer any singularity ($\omega = \pi$, $\lambda = 1$, $\beta = 0$) and the stress field remains bounded. Note however that, because the asymptotic expansions assume $d \neq 0$, μ tends to infinity as $\omega \to \pi$ as observed in Figure 9, not because of l but because $d \to 0$. By the way, it validates the hypothesis that l and d are of the same order of magnitude for a wide range of opening angles ω.

The above reasoning remains valid provided $l \approx d$ or even $l << d$, so that both l and d tend to 0 as $d \to 0$ (the parameter used to carry out the expansions governs). But one can also write the asymptotic expansions with respect to l with the dimensionless parameter $\xi = d / l = 1 / \mu$. This must give the same results from the theoretical point of view and would be better suited to large openings since it holds provided $l \approx d$ or even $d << l$, so that both l and d tend to 0 as $l \to 0$. Nevertheless, this approach contains additional numerical difficulties. Indeed, varying μ as previously done, i.e. the dimensionless crack length for a fixed radius of the damaged zone in the inner domain, can be easily carried out by buttoning nodes; whereas varying ξ, i.e. the damaged zone radius for a fixed dimensionless crack length, needs drastically refining the mesh in the vicinity of the corner to keep a sufficient number of elements within the damaged zone even if it becomes very small.

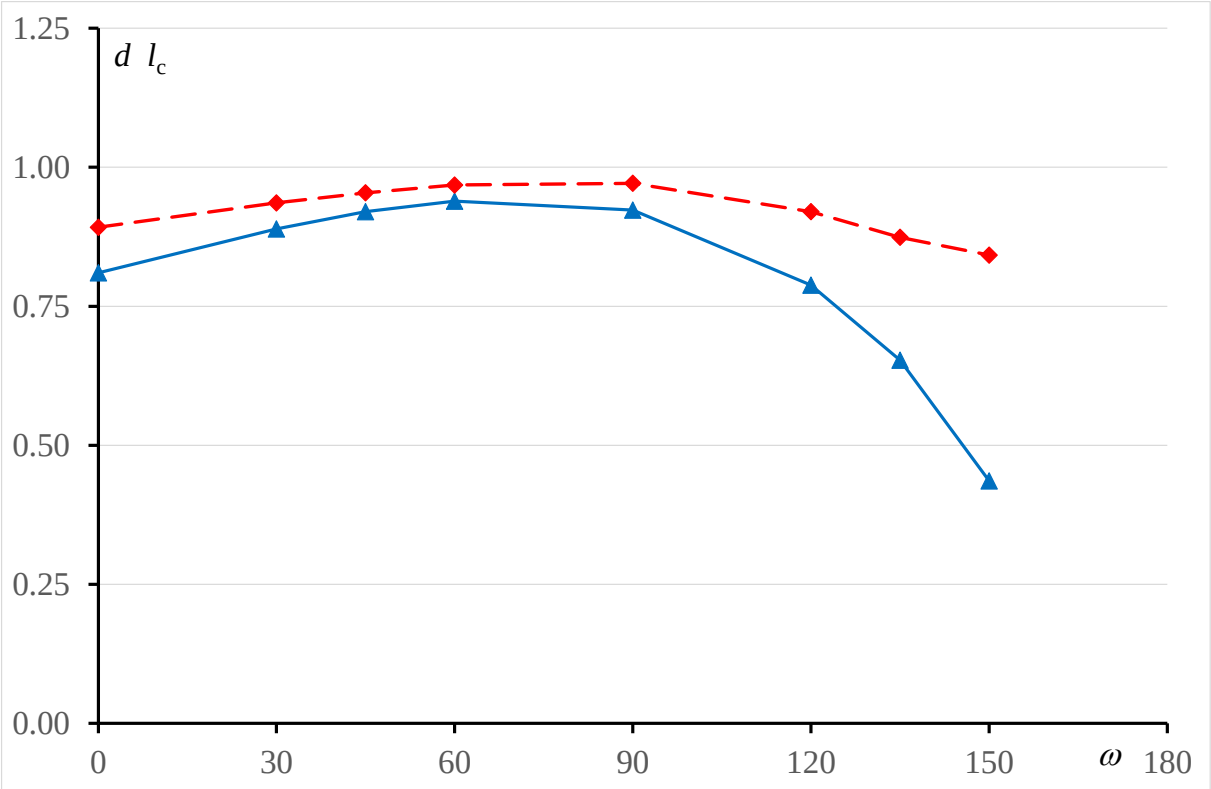

Figure 8. The damaged zone size d (mm) (blue solid line) (Eqn. (32)) and the critical crack length l_c (mm) (red dashed line) (Eqn. (48)) as functions of the opening angle ω (deg.).

As predicted by the coupled criterion in brittle materials, in this class of quasi-brittle materials, the virtual crack has a given length. This model differs substantially from fracture models based on damage laws where cracks, defined by a damage parameter reaching 1, arise more gradually.

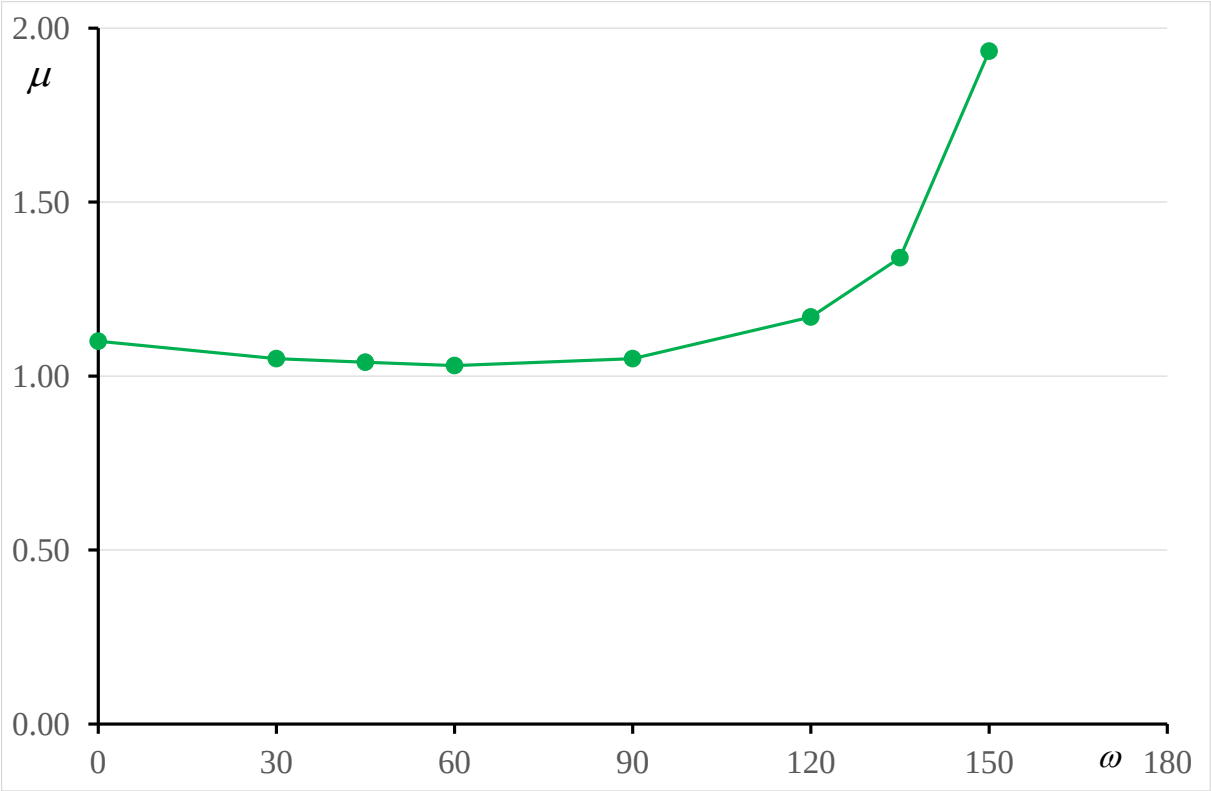

Figure 9. The dimensionless parameter $\mu = l / d$ as a function of the opening angle ω (deg.).

Obviously from Figure 9, $\mu > 1$ means that the crack extends beyond the boundary of the damaged zone. This is in agreement with the values of σ_c and $\sigma(d,0)$ (Eqn. (34)). A "damaged zone" may develop again at the tip of the crack extension, but this is out of the scope of this study which is only interested in the failure initiation and the crack is only a virtual one.

7.2 *Fixed opening* $\omega = \pi / 2$ *, fixed* σ_c *and* G_c *, variable* D_c

Again in that case $G_c'(r) = \mathcal{G}_c$. The best way to observe the convergence of the quasi-brittle solution toward the brittle one is to vary the parameter D_c (see (28)) which expresses the ability of the material to damage, the larger D_c, the smaller the damaged zone radius d (Figure 10). Simultaneously, $d \to 0$ and the critical crack length l_c converges toward the critical crack length l_0 in the brittle case. This convergence can also be observed in Figure 11 showing the GSIF in the quasi-brittle case k_c^{dam} approaching the GSIF k_c in the brittle case. Out of the domain spanned by D_c in Figures 10 and 11 (roughly from 0.06 to 0.6 MPa), the convergence of the two nested Newton algorithms becomes difficult to ensure.

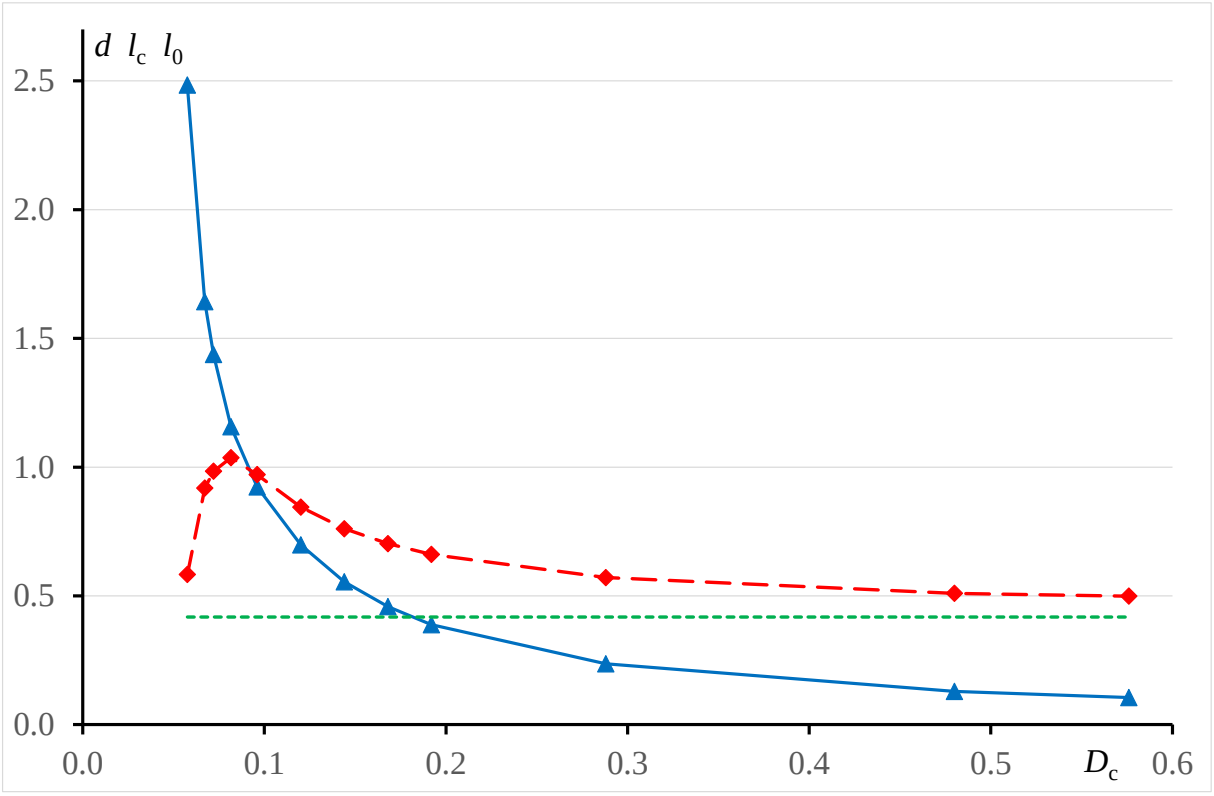

Figure 10. The damage zone radius d (mm) (blue solid line) (32) at crack initiation, the critical crack length l_c (mm) (red dashed line) (48) for the quasi-brittle material when D_c (MPa) varies, compared to the crack initiation length l_0 (mm) (13) (green dotted line) for the brittle material, for $\omega = \pi / 2$.

Note in Figure 10 the reverse trend on the crack length as the damaged zone becomes large (i.e. when D_c decreases) and the crack length becomes smaller than its radius. This occurs according to (34) because the threshold defined by the boundary of the damage zone becomes smaller than σ_c, it varies like $\sqrt{D_c}$.

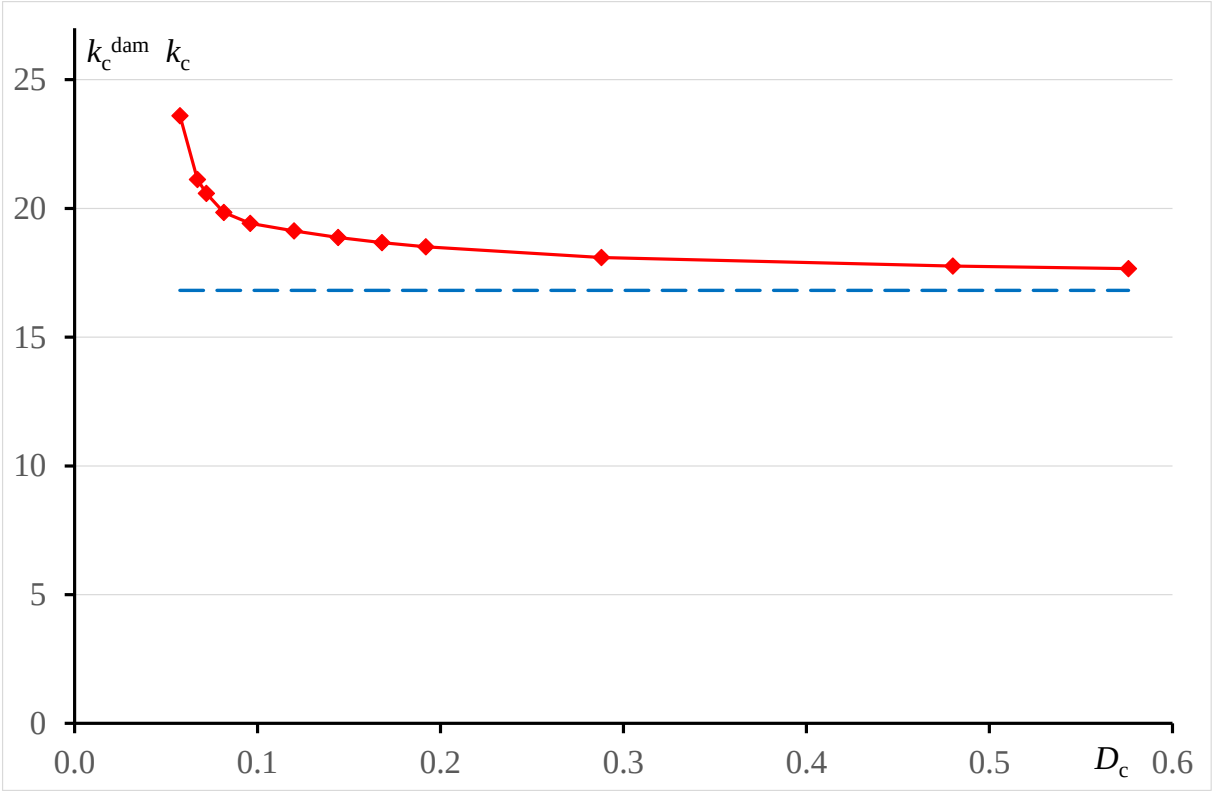

Figure 11. The GSIF k_c^{dam} (MPa mm$^{0.455}$) at failure (Eqn. (53)) (red solid line) compared to the critical value k_c (MPa mm$^{0.455}$) (Eqn. (13)) in the brittle material (blue dashed line) when D_c (MPa) varies, for $\omega = \pi / 2$.

7.3 *Fixed opening* $\omega = \pi / 2$, *fixed* D_c, *variable* σ_c *and* G_c

The main challenge in this section is to know how σ_c and G_c vary with the damage. This obviously plays a crucial role in the prediction of crack initiation. Alike the Young modulus, we assume for consistency that the strength and the toughness follow a power law within the damaged zone. They decrease as the damage increases (i.e. as the Young modulus decreases)

$$\sigma_c'(r) = \sigma_c \left(\frac{r}{d}\right)^{\gamma}, \quad G_c'(r) = \mathcal{G}_c \left(\frac{r}{d}\right)^{2\gamma} \text{ for } r \le d, \text{ with } \gamma \ge 0 \; ; \; \sigma_c'(r) = \sigma_c, \; G_c'(r) = \mathcal{G}_c \text{ otherwise} \quad (59)$$

The exponents γ and 2γ retains the ratio $G_c' / \sigma_c'^2$ unchanged, but other choices can be made. The decay hypothesis is based on a mechanism of damage by nucleation of micro-cracks and micro-voids, as described in (Mazars, 1986; Lemaitre and Chaboche, 1990) for example. Such a decay in strength was evoked in (Bazant and Planas, 1998), we extend it to toughness as it was predicted in porous materials if the porosity becomes large enough (Leguillon and Piat,

2008). This excludes ductile damage and fracture which are associated with large plastic deformations and where the hardening phenomenon can lead to very different results.

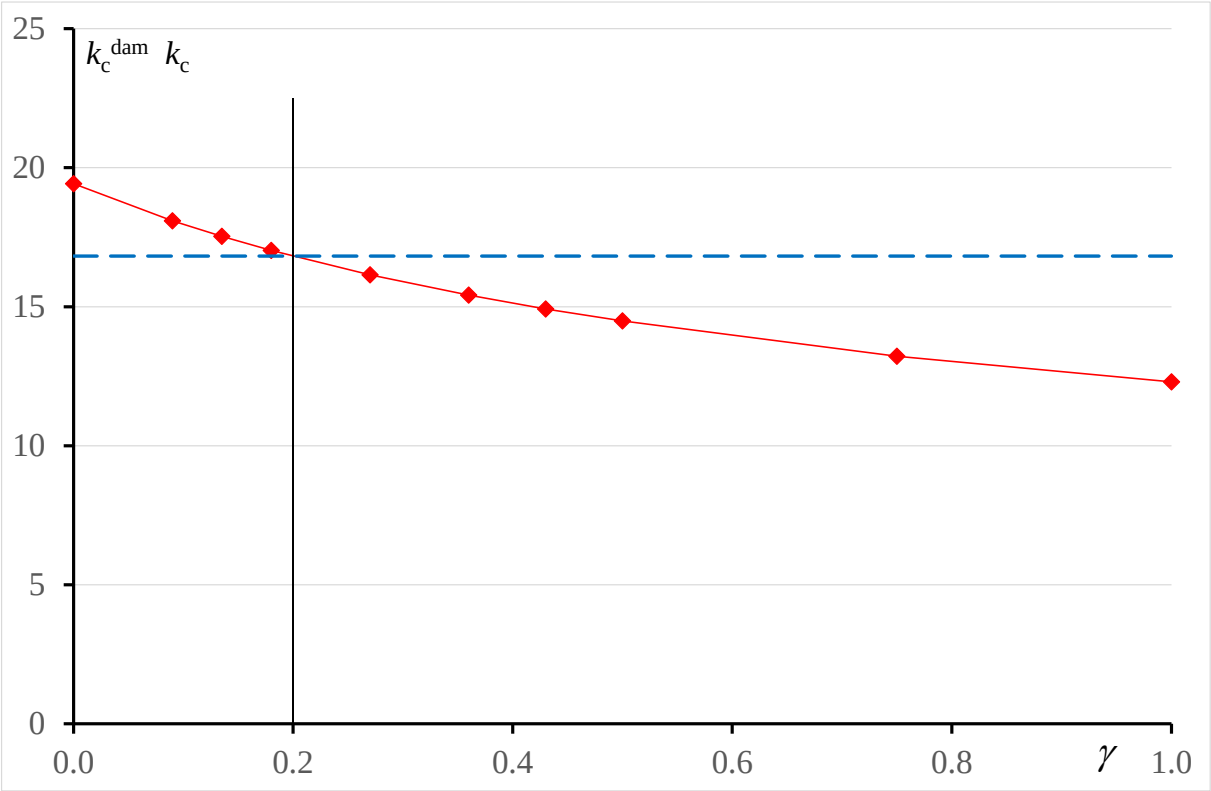

Figure 12. The critical GSIF k_c^{dam} (MPa mm$^{0.455}$) (red solid line) (quasi-brittle material) function of the dimensionless parameter γ compared to k_c (MPa mm$^{0.455}$) (blue dashed line) (brittle material), for $\omega = \pi / 2$.

Using the assumption (59), we compute k_c^{dam} as a function of γ and generate the graph $k_c^{dam}(\gamma)$ in Figure 12. Notice that, for $\gamma = 0.2$, then $k_c^{dam} = k_c$. For smaller values of γ , i.e. for fracture parameters only slowly decreasing, the damaged zone blunts the notch leading to an apparent higher strength, whereas if the fracture parameters decrease faster, then there is a weakening of the structure. For instance, for $\gamma = \beta = 0.72$ (i.e. a unique power law to describe both the stiffness and the fracture properties change due to damage), $k_c^{dam} = 13.3$ MPa mm$^{0.455}$ far below $k_c = 16.8$ MPa mm$^{0.455}$.

The ratio between the critical crack length l_c and the radius d of the damaged area remains almost the same as if $G_c'(r)$ and $\sigma_c'(r)$ are constant, as shown in Figure 13.

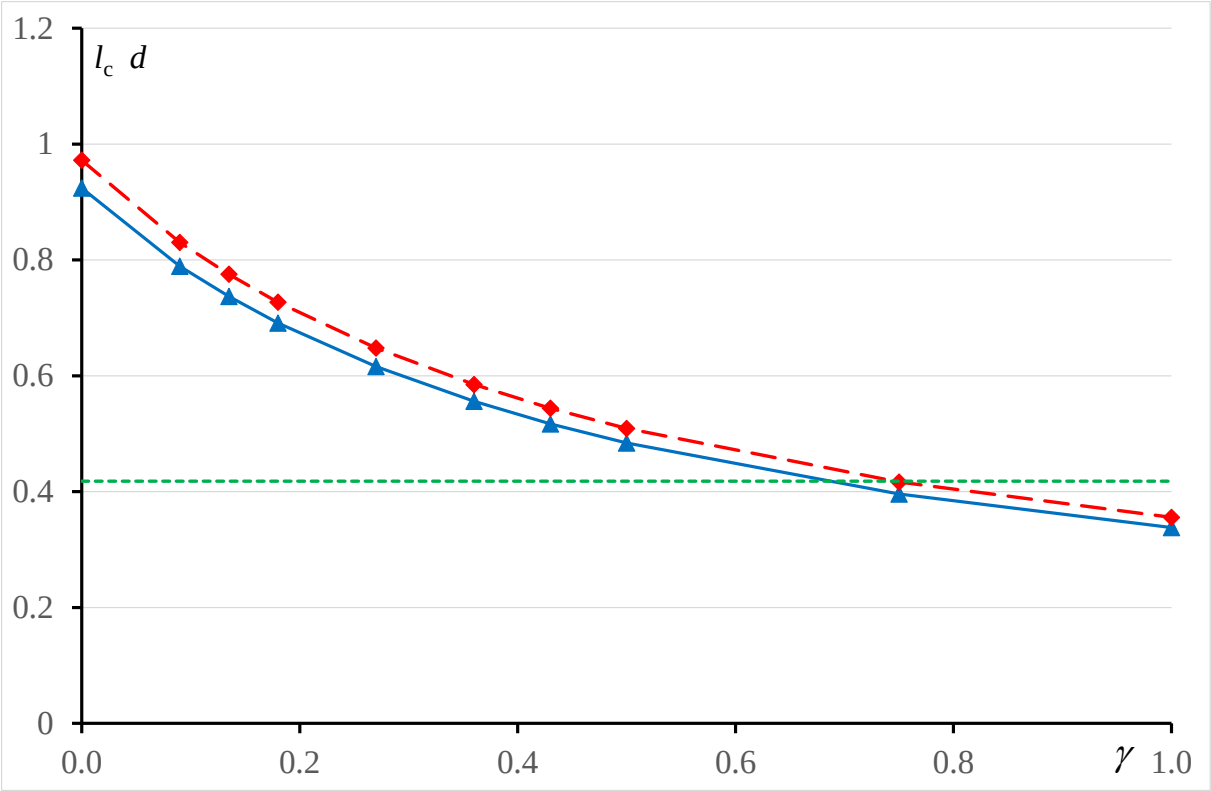

Figure 13. The damaged zone radius d (mm) (blue solid line) and the critical crack length l_c (mm) (red dashed line) compared to the critical crack length l_0 (mm) (green dotted line) for the dimensionless varying parameter γ.

7.4 *Determination of* d *and identification of* D_c

In the absence of full-field measurements we may approximate $\underline{U}^{DIC}$ by FE in a V-notched specimen (opening angle $\omega = \pi / 2$) under three-point bending loading (Figure 14) with various damaged zone radii: 0.1, 0.2, 0.5 and 1 mm (recall that in the damage zone $E' = (r / d)^{\beta} E$ with $\beta =$ 0.72). Of course, the mesh is strongly refined in the vicinity of the notch in order to well capture the damaged zone. Note that, here d is a priori fixed and the aim of the calculation is to check the ability of the method described in Section 5 to determine its value.

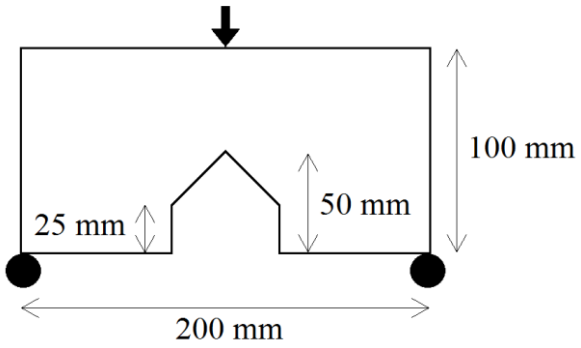

Figure 14. The specimen used to simulate by FE the displacement field that could be obtained by DIC. Computations are carried out on one half of the specimen due to symmetry.

The coefficients k (1) and k^- (39) are calculated using the path independent integral Ψ (Appendix 1) along 3 different paths located between 5 and 10 mm from the notch root, i.e. rather far from the damaged zone itself, and averaged (thus, a DIC picture of 20 × 20 mm^2 around the notch root would largely suffice). To prevent crack initiation, one needs only to ensure that the load is below the threshold, i.e. $k < k_c^{\mathrm{dam}}$. A prescribed displacement of 0.1 mm at point A leads to $k = 11.6$ MPa mm$^{0.455}$. According to (40) and (41), the determination of the damaged zone size d and the identification of the damage parameter D_c are shown in Table 1.

Table 1. Determination of the damaged zone size d and identification of the damage parameter D_c from a FE simulation of a DIC displacement field for $\omega = \pi / 2$. It is recalled that $\lambda = 0.545$, $\kappa = 0.624$, $L^* = LE = 1.417$, $\tilde{L} = -4.929$.

d (mm)	0.1	0.2	0.5	1
k (MPa mm$^{0.455}$)	11.6	11.6	11.6	11.6
k^- (MPa mm$^{1.545}$)	− 4.67	− 9.94	− 26.95	− 57.30
d (mm) from (40)	0.100	0.201	0.502	1.003
D_c (MPa) from (41)	0.257	0.137	0.059	0.032

Obviously the determination of d turns out to be excellent, the error is less than 0.5%. This feature was already reported by Leguillon (2011) in a slightly different context: the determination of the length of a short crack. In this reference the robustness of this approach was tested by polluting the FE displacement field with a white noise and it was observed that the results remained very satisfactory.

Once d is accurately known, D_c is straightforwardly derived according to (41). Of course, D_c is a material constant, the various values exhibited in line 5 of Table 1 are interpreted as follows, say for row 4: $D_c = 0.059$ MPa will cause a damaged zone size $d = 0.5$ mm if a displacement of 0.1 mm is prescribed at the load pin.

9. Conclusion

The damage law presented herein (Sections 3 and 4) although not traditional (i.e. based on the definition of an internal variable, the thermo-dynamic associated force and a dissipation potential), enjoys the main features of a usual damage law: the Young modulus decreases, the stress field remains bounded, the damage zone is defined by a threshold and the mechanism dissipates energy. It seems appropriate to quasi-brittle materials, no diffuse damage may arise following this law. The material parameter D_c characterizing this law can be identified using an asymptotic procedure based on a full-field measurement of the displacements.

The coupling of this damage law with the so-called coupled criterion provides a method to predict failure initiation at V-notches for a wide class of quasi-brittle materials. As in brittle materials, the crack suddenly appears, in contrast to models of damage where it arises gradually. Based on some assumptions, the influence of the decaying tensile strength and material toughness in the damaged zone is studied. Moreover, it is shown that the coupled criterion (Section 2) can still be used, neglecting the damage zone, by an appropriate change in the actual toughness.

Clearly the choices that have been made are closely related to damage and crack nucleation at the root of a sharp notch, a source of failure in structures. Both the damage law and the coupled criterion are based on Williams' expansions applicable to this case. Generalization to other situations may prohibit the use of semi-analytical expressions, however, such generalization may require FE computations. The key point is two mechanisms (damage and crack nucleation) that are weakly coupled. Crack nucleation is not a direct consequence of the evolution of the damage parameter reaching a threshold (often the limit value 1), but it is superimposed. The weal coupling is because the damage locally modifies the material parameters and thus influences the onset of the crack. Then, two nested loop can be used: an outer one analyzes the evolution of the material parameters resulting of any damage law using FE computations, while the inner one implements the CC in this context, again using FE computations (Martin and Leguillon, 2004). One can refer for instance to (Leguillon et al.,

2016) where the oxidation of the polymer evolves with time, thus modifying the conditions for the appearance of surface cracks.

The assumption of a decrease of the Young modulus to describe the damage is commonly admitted and it seems realistic to apply to materials sensitive to damage like some polymers. But an important class of quasi-brittle materials is formed of metals where a small plastic zone develops at the root of the V-notch (small scale yielding). Obviously, the case of plasticity spreading all over the specimen is excluded from the present analysis. In the case of small scale yielding, the Young modulus can be considered as the secant modulus of a non-linear constitutive law and its variation following a power law has some analogies with the Ramberg-Osgood plastic law. It remains a good approximation provided no unload occurs. However, it is difficult to go further in this direction. In particular, the boundary of the plastic zone (i.e. herein the damaged zone) is not defined by a yield strength but by a function, indeed independent of the applied load, but varying with θ (see Eqn. (35)) which seems incompatible with classical plastic laws. Thus, we plan to extend the study to cover a wider range of quasi-brittle materials including materials undergoing small scale yielding.

Validation of the proposed failure initiation criterion for hard metals undergoing a small scale yielding is planned in a future publication.

Acknowledgements: Zohar Yosibash acknowledges the ISF grant # 593/14.

References

Appel T., Merhmann V., Watkins D., 2002. Structured eigenvalue methods for the computation of corner singularities in 3D anisotropic elastic structures, Comp. Meth. Appl. Mech. Engng. 191, 4459-4473.

Bazant Z.P., Planas J., 1998. Fracture and size effect in concrete and other quasi-brittle materials, CRC Press, Boca Raton, USA.

Camanho P., Erçin G., Catalanotti G., Mahdi S., Linde P., 2012. A finite fracture mechanics model for the prediction of the open-hole strength of composite laminates. Compos. A: Appl. Sci. Manuf. 43, 1219-1225.

Carpinteri A., Cornetti P., Sapora A., 2012. A Finite Fracture Mechanics approach to the asymptotic behaviour of U-notched structures, Fatigue Fract. Eng. Mater. Struct. 35, 451-457.

Carrere N., Martin E., Leguillon D., 2015. Comparison between models based on a coupled criterion for the prediction of the failure of adhesively bonded joints, Eng. Fract. Mech. 138, 185-201.

Cornetti P., Pugno N., Carpinteri A., Taylor D., 2006. Finite fracture mechanics: a coupled stress and energy failure criterion, Eng. Fract. Mech. 73, 2021-2033.

García I., Mantic V., Blázquez A., París F., 2014. Transverse crack onset and growth in cross-ply [0/90]s laminates under tension. Application of a coupled stress and energy criterion, Int. J. Solids Struct. 51, 3844-3856.

García I., Mantic V., Graciani E., 2015. A model for the prediction of debond onset in spherical-particle-reinforced composites under tension. Application of a coupled stress and energy criterion, Compos. Sci. Technol. 106, 60-67.

Hebel J., Becker W., 2008. Numerical analysis of brittle crack initiation at stress concentrations in composites, Mech. Adv. Mater. Struct. 15, 410-420.

Hebel J., Dieringer R., Becker W., 2010. Modeling brittle crack formation at geometrical and material discontinuities using a Finite Fracture Mechanics approach. Eng. Fract. Mech. 77, 3558-3572.

Hell S., Weissgraeber P., Felger J., Becker W., 2014. A coupled stress and energy criterion for the assessment of crack initiation in single lap joints: A numerical approach, Eng. Fract. Mech. 117, 112-126.

Henninger C., Roux S., Hild F., 2010. Enriched kinematic fields of cracked structures. Int. J. Solids Structures 47, 3305-3316.

Hild F., Roux S., 2006. Digital image correlation: from displacement measurement to identification of elastic properties – a review. Strain 42, 69-80.

Hutchinson J.W., 1968. Singular behaviour at the end of a tensile crack in a hardening material, J. Mech. Phys. Solids 16, 13-31.

Kachanov L., 1958. On the creep rupture time (in Russian), Izv AN SSSR, Otd. Tehn. Nauk. 8, 26-31.

Kachanov L, 1986. Introduction to continuum damage mechanics, Springer Science, Dordrecht.

Labossiere P.E.W., Dunn M.L., 1998. Calculation of stress intensities at sharp notches in anisotropic media, Engng. Fract. Mech. 61, 635-654.

Leguillon D., 1989. Calcul du taux de restitution de l'énergie au voisinage d'une singularité, C.R. Acad. Sci. Paris, 309, série II, 1989, 945-950.

Leguillon D., 2002. Strength or toughness? A criterion for crack onset at a notch, Eur. J. Mech. A/Solids 21, 61-72.

Leguillon D., 2008. A damage model based on singular elastic fields, C.R. Mécanique 336, 283-288.

Leguillon D., 2011. Determination of the length of a short crack at a v-notch from a full field measurement, Int. J. Solids Structures 48, 884-892.

Leguillon D., Lafarie-Frenot M.C., Pannier Y., Martin E., 2016. Prediction of the surface cracking pattern of an oxidized polymer induced by residual and bending stresses, Int. J. Solids Structures (in press).

Leguillon D., Piat R., 2008. Fracture of porous materials - Influence of the pore size, Engng. Fract. Mech. 75, 1840-1853.

Leguillon D., Quesada D., Putot C., Martin E., 2007. Size effects for crack initiation at blunt notches or cavities, Engng. Fract. Mech. 74, 2420-2436.

Leguillon D., Sanchez-Palencia E., 1987. Computation of Singular Solutions in Elliptic Problems and Elasticity, John Wiley & Sons/Masson, New York/Paris.

Leguillon D., Yosibash Z., 2003. Crack onset at a v-notch. Influence of the notch tip radius, Int. J. Fract. 122, 1-21.

Lemaitre J., Chaboche J.L., 1990. Mechanics of solid materials, Cambridge University Press, Cambridge UK.

Martin E., Leguillon D., 2004. Energetic conditions for interfacial failure in the vicinity of a matrix crack in brittle matrix composites, Int. J. Solids Structures 41, 6937-6948.

Martin E., Leguillon D., Carrere N., 2010. A twofold strength and toughness criterion for the onset of free-edge shear delamination in angle-ply laminates, Int. J. Solids Structures 47, 1297-1305.

Martin E., Leguillon D., Carrere N., 2012. A coupled strength and toughness criterion for the prediction of the open hole tensile strength of a composite plate, Int. J. Solids Structures 49, 3915-3922.

Mazars J., 1986. A descriptions of micro- and macroscale damage of concrete structures, Engng. Fract. Mech. 25, 729-737.

Moes N., Stolz C., Bernard P.E., Chevaugeon N., 2011. A level set based model for damage growth: the thick level set approach, Int. J. Numer. Meth. Engng. 86, 358-380.

Moradi A., Carrere N., Leguillon D., Martin E., Cognard J-Y., 2013. Strength prediction of bonded assemblies using a coupled criterion under elastic assumptions: effect of material and geometrical parameters, Int. J. of Adhesion & Adhesives 47, 73-82.

Picard D., Leguillon D., Putot C., 2006. A method to estimate the influence of the notch-root radius on the fracture toughness of ceramics, J. Eur. Ceram. Soc. 26, 1421-1427.

Priel E., Yosibash Z., Leguillon D., 2008. Failure initiation at a blunt V-notch tip under mixed mode loading, Int. J. Fracture 149, 143-173.

Quesada D., Picard D., Putot C., Leguillon D., 2009. The role of the interbed thickness on the step-over fracture under overburden pressure, Int. J. Rock Mech. and Min. Sci. 46, 281-288.

Rice J.R., 1968. Mathematical Analysis in the Mechanics of Fracture, in Fracture, H. Liebowitz (ed.), Vol 2, Academic Press, New York, pp. 191-311.

Rice J.R., Rosengren G.F., 1968. Plane strain deformation near a crack tip in a power-law hardening material, J. Mech. Phys. Solids 16, 1-12.

Romani R., Bornert M., Leguillon D., Le Roy R., Sab K., 2015. Detection of crack onset in double cleavage drilled specimens of plaster under compression by digital image correlation. Eur. J. mech. A/Solids, 51, 172-182.

Sapora A., Cornetti P., Carpinteri A., 2013. A Finite Fracture Mechanics approach to V-notched elements subjected to mixed-mode loading, Eng. Fract. Mech. 97, 216-226.

Van Dyke M. 1964. Perturbation methods in fluid mechanics, Academic Press, New York.

Weissgraeber P., Leguillon D., Becker W., 2016. A review of Finite Fracture Mechanics: Crack initiation at singular and non-singular stress-raisers, Arch. Appl. Mech., 86, 375-401.

Williams M.L., 1959. The stress around a fault or crack in dissimilar media, Bul. Seismol. Soc. America 49, 199-204.

Yosibash Z., Priel E., Leguillon D., 2006. A failure criterion for brittle elastic materials under mixed-mode loading, Int. J. Fract. 141, 289-310.

Yosibash Z., 2012. Singularities in elliptic boundary value problems and elasticity and their connection with failure initiation, Interdisciplinary Applied Mathematics 37, Springer, New-York.

Appendix 1

For more details in this appendix refer to (Leguillon and Sanchez-Palencia, 1987). The eigenpair λ and $\underline{u}(\theta)$ in (1) is solution to the eigenvalue problem

$$\left[-\lambda^2\mathbf{A}+\lambda(\mathbf{B}-\mathbf{B}^{\mathrm{T}})+\mathbf{C}\right]\underline{u}=0 \qquad \text{(A1.1)}$$

where **A** and **C** are symmetric operators and $\mathbf{B}-\mathbf{B}^{\mathrm{T}}$ is skew symmetric. In (1), λ is the smallest positive solution to (A1.1). The eigenpair $(\lambda,\underline{u})$ depends only on the opening angle ω, for a traction free V-notch λ is a real number such that $0.5\le\lambda\le 1$ ($\lambda=0.5$ for a crack, $\omega=0$; $\lambda=1$ for a straight edge, $\omega=\pi$), thus $\underline{\underline{\varepsilon}}$ and $\underline{\underline{\sigma}}\to\infty$ as $r\to 0$ (except of course if $\lambda=1$). Details on the computation of the eigenpairs are given in (Leguillon and Sanchez-Palencia, 1987; Yosibash 2012).

The generalized stress intensity factor *k* of the singular term $r^{\lambda}\underline{u}(\theta)$ in (1) can be extracted from a FE computed solution $\underline{U}^{\mathrm{FE}}$ (an approximation of $\underline{U}$ in (1)) thanks to the path independent integral Ψ (Leguillon and Sanchez-Palencia, 1987; Labossiere and Dunn, 1998)

$$k=\frac{\Psi(\underline{U}^{\mathrm{FE}},r^{-\lambda}\underline{u}^{-})}{\Psi(r^{\lambda}\underline{u},r^{-\lambda}\underline{u}^{-})} \quad \text{with } \Psi(\underline{\varphi},\underline{\psi})=\frac{1}{2}\int_{\Gamma}\left[\underline{\underline{\sigma}}(\underline{\varphi}).\underline{n}.\underline{\psi}-\underline{\underline{\sigma}}(\underline{\psi}).\underline{n}.\underline{\varphi}\right]\mathrm{d}s \qquad \text{(A1.2)}$$

The line Γ is any contour encompassing the notch root, starting and ending on the traction free edges of the notch, and $\underline{n}$ is its normal pointing toward the origin. The path independence is ensured provided the functions $\underline{\varphi}$ and $\underline{\psi}$ fulfil the equilibrium equations with 0 right hand side member (vanishing momentum equation and stress free boundary conditions). The pair $(-\lambda,\underline{u}^{-})$ is also an eigenpair, so-called dual eigen-pair to $(\lambda,\underline{u})$ (Leguillon and Sanchez-Palencia, 1987; Yosibash, 2012). It is a mathematical solution to (1), however since it has an unbounded energy at the V-notch tip, it cannot serve as a "physical solution" to the elasticity problem. It is sometimes baptized super-singular mode (Henninger et al., 2010). A physical interpretation can be provided to the dual eigenpair in problems formulated in unbounded domains (Leguillon, 2011).

Appendix 2

The change in potential energy between the uncracked and cracked states $-\Delta \mathcal{W}^{\mathrm{P}}$ in Section 2 can be expressed in terms of the integral Ψ (Appendix 1)

$$-\Delta \mathcal{W}^{\mathrm{P}} = \frac{1}{2}\int_{\Gamma}\left[\underline{\underline{\sigma}}(\underline{U}^{l}).\underline{n}.\underline{U}^{0} - \underline{\underline{\sigma}}(\underline{U}^{0}).\underline{n}.\underline{U}^{l}\right]\mathrm{d}s = \Psi\left(\underline{U}^{l},\underline{U}^{0}\right) \tag{A2.1}$$

where $\underline{U}^{l}$ and $\underline{U}^{0}$ are the elastic solutions respectively with and without a crack of length l and where Γ is a contour (Appendix 1) encompassing a domain containing the crack in the vicinity of the notch root. Using the change of variable $y_i = x_i / l$ ($\rho = r / l$), the above integral (A2.1) can be rewritten in the inner domain Ω_{in} (stretched by $1/l$). Then using the inner expansions

$$\begin{aligned}
&\underline{U}^{0}(x_1, x_2) = \underline{U}^{0}(ly_1, ly_2) = \underline{R} + kl^{\lambda}\rho^{\lambda}\underline{u}(\theta) + \ldots \\
&\underline{U}^{l}(x_1, x_2) = \underline{U}^{l}(ly_1, ly_2) = \underline{R} + kl^{\lambda}\left[\rho^{\lambda}\underline{u}(\theta) + \underline{\hat{V}}^{1}(y_1, y_2)\right] + \ldots
\end{aligned} \tag{A2.2}$$

into (A2.1), using some properties of independence with respect to the integration path leads to

$$\begin{aligned}
&-\Delta \mathcal{W}^{\mathrm{P}} = k^2 l^{2\lambda}\psi\left(\underline{\hat{V}}^{1}, \rho^{\lambda}\underline{u}(\theta)\right) = k^2 l^{2\lambda}\psi\left(\underline{V}^{1}, \rho^{\lambda}\underline{u}(\theta)\right) = Ak^2 l^{2\lambda} \\
&\text{with } A = \psi\left(\underline{\hat{V}}^{1}, \rho^{\lambda}\underline{u}(\theta)\right)
\end{aligned} \tag{A2.3}$$

The same reasoning can be applied in Section 4 where the perturbation of the domain is no longer a small crack but a small damaged area. The analogue to (A2.1) is

$$-\Delta \mathcal{W}^{\mathrm{D}} = \frac{1}{2}\int_{\Gamma}\left[\underline{\underline{\sigma}}(\underline{U}^{d}).\underline{n}.\underline{U}^{0} - \underline{\underline{\sigma}}(\underline{U}^{0}).\underline{n}.\underline{U}^{d}\right]\mathrm{d}s = \Psi\left(\underline{U}^{d},\underline{U}^{0}\right) \tag{A2.4}$$

It is the change in potential energy between the damaged and the undamaged structure. Again, the change of variable $z_i = x_i / d$ ($\zeta = r / d$) allows rewriting (A2.4) in the inner domain and using the inner expansions of $\underline{U}^d$ and $\underline{U}^0$ (see Eqn. (22)) leads to

$$-\Delta \mathcal{W}^{\mathrm{D}} = k^2 d^{2\lambda} \psi\left(\underline{\hat{W}}^1, \zeta^\lambda \underline{u}(\theta)\right) = k^2 d^{2\lambda} \psi\left(\underline{W}^1, \zeta^\lambda \underline{u}(\theta)\right) = L k^2 l^{2\lambda}$$
$$\text{with L} = \psi\left(\underline{\hat{W}}^1, \zeta^\lambda \underline{u}(\theta)\right) \tag{A2.5}$$

Finally, the function $B(\mu)$ in (45) (Section 6) is determined using the same procedure. The inner domain embeds the damage zone $\Omega_{\mathrm{d,in}}$ with radius 1 and a crack emanating from the notch root with dimensionless length $\mu = l / d$. In our FE computations, this length is varied from 0 to 2 by inserting double nodes and

$$B(\mu) = \Psi\left(\underline{\hat{W}}^1, \zeta^\lambda \underline{u}(\theta)\right) = \Psi\left(\underline{W}^1, \zeta^\lambda \underline{u}(\theta)\right) \tag{A2.6}$$

where, according to (44), $\underline{W}^1$ and $\underline{\hat{W}}^1$ depend on μ and where the integration path encompasses the damage zone and the crack (which length can be larger than the damaged zone).

Appendix 3

Let us consider the stretched domain Ω_{in} (stretched by 1/*d*) so the radius of the damaged zone is 1 (see Figure A2-1). In this domain $\underline{W}^1(z_1, z_2) = \zeta^\lambda \underline{u}(\theta) + \underline{\hat{W}}^1(z_1, z_2)$, given in (24) (Section 4), is the solution to the elasticity system so it has to satisfy the equilibrium equation and boundary conditions (see also the appendix in (Leguillon, 2002)).

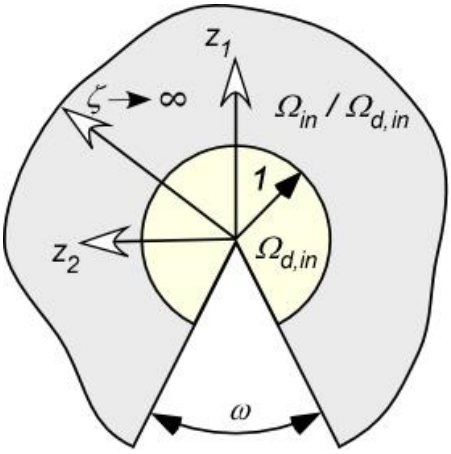

Figure A2-1. The unbounded domain embedding the damage zone with radius 1.

Since there are two domains such that in each the Young' modulus is different, then the stress tensor in each is given by a different expression

$$\begin{cases} \underline{\underline{\sigma}}_z(\underline{W}^1) = \mathbf{C} : \nabla_z(\underline{W}^1) \text{ in } \Omega_{\text{in}} \setminus \Omega_{\text{d,in}} \\ \underline{\underline{\sigma}}_z(\underline{W}^1) = \mathbf{C}' : \nabla_z(\underline{W}^1) \text{ in } \Omega_{\text{d,in}} \end{cases} \tag{A3.1}$$

where ∇_z denotes the gradient with respect to the space variables $z_i = x_i / d$ ($\zeta = r / d$) which span the unbounded space Ω_{in} as $d \to 0$ (Figure 1) and $\mathbf{C}$ and $\mathbf{C}'$ are the fourth order stiffness tensors relying respectively on E and E' and ν. The same relationships (A2.1) hold for $\underline{\hat{W}}^1$.

Substituting (A3.1) in the equilibrium equations, one obtains:

$$\begin{cases} -\nabla_z . \underline{\underline{\sigma}}_z(\underline{W}^1) = 0 \text{ in } \Omega_{\text{in}} \\ \underline{\underline{\sigma}}_z(\underline{W}^1).\underline{n} = 0 \text{ on } \partial\Omega_{\text{in}} \\ \underline{W}^1(z_1, z_2) \cong \zeta^{\lambda}\underline{u}(\theta) \\ \underline{W}^1 \text{ and } \underline{\underline{\sigma}}_z(\underline{W}^1).\underline{N} \text{ are continuous through the interface I} \end{cases} \tag{A3.2}$$

The boundary $\partial\Omega_{\text{in}}$, with the outer normal $\underline{n}$, embeds the two unbounded edges of the V-notch, $\Omega_{\text{d,in}}$ is the stretched damage zone with radius 1, I is the interface between the domains

Ω_{in} and $\Omega_{d,in}$ and and $\underline{N}$ its normal pointing toward the notch root. The symbol $\cong$ means "behaves like at infinity", ζ and θ are the polar coordinates in Ω^{in}.

Using the superposition principle

$$\underline{W}^1(z_1, z_2) = \zeta^\lambda \underline{u}(\theta) + \underline{\hat{W}}^1(z_1, z_2) \tag{A3.3}$$

It comes immediately that $\underline{\hat{W}}^1$ is solution to the following problem

$$\begin{cases} -\nabla_z . \underline{\underline{\sigma}}_z(\underline{\hat{W}}^1) = 0 \ \text{ in } \Omega_{in} \setminus \Omega_{d,in} \\ -\nabla_z . \underline{\underline{\sigma}}_z(\underline{\hat{W}}^1) = \nabla_z . \left(\mathbf{C}' : \nabla_z \left(\zeta^\lambda \underline{u}(\theta) \right) \right) \ \text{ in } \Omega_{d,in} \\ \underline{\underline{\sigma}}_z(\underline{\hat{W}}^1).\underline{n} = 0 \ \text{ on } \partial\left(\Omega_{in} \setminus \Omega_{d,in}\right) \\ \underline{\underline{\sigma}}_z(\underline{\hat{W}}^1).\underline{n} = -\mathbf{C}' : \nabla_z \left(\zeta^\lambda \underline{u}(\theta) \right) \ \text{ on } \partial\Omega_{d,in} \cap \partial\Omega_{in} \\ \underline{\hat{W}}^1(z_1, z_2) \cong 0 \\ \underline{\hat{W}}^1 \text{ and } \underline{\underline{\sigma}}_z(\underline{\hat{W}}^1).\ \underline{N} \text{ continuous through I} \end{cases} \tag{A3.4}$$

The continuity of $\underline{\underline{\sigma}}_z(\underline{\hat{W}}^1).\underline{N}$ through the interface I is a consequence of the following transmission condition knowing that $\mathbf{C} = \mathbf{C}'$ on the interface

$$\left[\!\left[\underline{\underline{\sigma}}_z(\underline{\hat{W}}^1) \right]\!\right].\ \underline{N} = -\left(\mathbf{C} - \mathbf{C}'\right) : \nabla_z \left(\zeta^\lambda \underline{u}(\theta) \right).\ \underline{N} \tag{A3.5}$$

where the bracket $[\![\ ]\!]$ holds for the discontinuity through the interface I, $\nabla_z \left(\zeta^\lambda \underline{u}(\theta) \right)$ is calculated at points located on this interface, what is possible knowing that this singular term has an analytical expression, refer for instance to (Yosibash, 2012).

Green's formula applied to $\underline{\hat{W}}^1$ in the domain $\Omega_{d,in}$ allows proving that the corresponding problem is well-posed. One has just to check that the resultant force and moment vanish as a consequence of the properties of the singular term $\zeta^\lambda \underline{u}(\theta)$ in the unperturbed (i.e. defined by $\mathbf{C}$ deriving from E and ν) and unbounded V-notched domain.

When the domain Ω_{in} embeds in addition a crack (Section 6), one has simply to add the following conditions on the two faces C_+ and C_- of the crack

$$\begin{cases} \underline{\underline{\sigma}}_z(\underline{W}^1).\underline{m} = 0 \text{ on } C_+ \cup C_- \\ \underline{\underline{\sigma}}_z(\underline{\hat{W}}^1).\underline{m} = -\mathbf{C} : \nabla_z\left(\zeta^\lambda \underline{u}(\theta)\right).\underline{m} \text{ on } \left(C_+ \cup C_-\right) \cap \left(\Omega_{in} \setminus \Omega_{d,in}\right) \\ \underline{\underline{\sigma}}_z(\underline{\hat{W}}^1).\underline{m} = -\mathbf{C}' : \nabla_z\left(\zeta^\lambda \underline{u}(\theta)\right).\underline{m} \text{ on } \left(C_+ \cup C_-\right) \cap \Omega_{d,in} \end{cases} \quad \text{(A3.6)}$$

where $\underline{m}$ denotes the outer normal to the crack faces C_+ and C_-.

Appendix 4

A classical and simple theory of damage in elastic materials (Kachanov, 1958, 1986; Marigo, 1981; Lemaitre and Chaboche, 1990) consists in the definition of the free energy density $\mathcal{W}^F$ (herein the strain energy density) as a function of two internal variables: the strain tensor $\underline{\underline{\varepsilon}}$ and the scalar damage variable δ

$$\mathcal{W}^F(\underline{\underline{\varepsilon}}, \delta) = \frac{1}{2}(1-\delta)\mathbf{C} : \underline{\underline{\varepsilon}} : \underline{\underline{\varepsilon}} \quad \text{(A4.1)}$$

where $\mathbf{C}$ is the stiffness Hooke tensor of the undamaged material relying on the Young modulus E and the Poisson ratio ν. Two constitutive laws are derived from this potential (using standard notations in damage mechanics)

$$\underline{\underline{\sigma}} = \frac{\partial \mathcal{W}^F}{\partial \underline{\underline{\varepsilon}}} = (1-\delta)\mathbf{C} : \underline{\underline{\varepsilon}} \text{ and } Y = -\frac{\partial \mathcal{W}^F}{\partial \delta} = \frac{1}{2}\mathbf{C} : \underline{\underline{\varepsilon}} : \underline{\underline{\varepsilon}} \quad \text{(A4.2)}$$

where as usual $\underline{\underline{\sigma}}$ is the stress tensor and Y is the thermodynamic force associated to δ that governs its evolution. Then the damage law takes the general form, based on the existence of a threshold Y_c

$$\begin{cases} Y < Y_c \;\Rightarrow\; \dot{\delta}=0 \\ Y = Y_c \;\Rightarrow\; \dot{\delta} \geq 0 \end{cases} \tag{A4.3}$$

where $\dot{\delta}$ is the time derivative of δ. According to Clausius-Duheim second principle of thermodynamics, damage can only grow. As a consequence, the density of energy dissipated to reach the damaged state defined locally by δ is

$$\mathcal{D} = \delta \; Y_c \tag{A4.4}$$

In the present paper, the material parameter D_c was introduced in Section 4 as the scaling coefficient defining the energy required to damage the material and more precisely to decrease the Young modulus E by ΔE in a surface ΔS, it is rewritten

$$\frac{\Delta \mathcal{W}}{\Delta S} = D_c \frac{\Delta E}{E} \tag{A4.5}$$

It is the density of energy consumed to damage the material. Following the classical formalism of the above damage law, the current Young modulus E' is such that

$$E' = E - \Delta E = E(1-\delta) \;\text{ and then }\; \delta = \frac{\Delta E}{E} \tag{A4.6}$$

Thus comparing (A4.4) and (A4.5) leads to

$$D_c = Y_c \tag{A4.7}$$